

BAW-2128, Rev. 1

May 1992

ANALYSIS OF CAPSULE OCIII-D
DUKE POWER COMPANY
OCONEE NUCLEAR STATION UNIT-3

-- Reactor Vessel Material Surveillance Program --

9206160242 920608
PDR ADDCK 05000287
P PDR

BW B&W NUCLEAR
SERVICE COMPANY

BAW-2128, Rev. 1

May 1992

ANALYSIS OF CAPSULE OCIII-D
DUKE POWER COMPANY
OCONEE NUCLEAR STATION UNIT-3

-- Reactor Vessel Material Surveillance Program --

by

A. L. Lowe, Jr., PE
J. D. Aadland
A. D. Nana
M. A. Rutherford
W. R. Stagg

B&W Document No. 77-2128-01
(See Section 11 for document signatures)

B&W Nuclear Service Company
Engineering and Plant Services Division
P. O. Box 10935
Lynchburg, Virginia 24506-0935

BW B&W NUCLEAR
SERVICE COMPANY

SUMMARY

This report describes the results of the examination of the third capsule (OCIII-D) of the Duke Power Company's Oconee Nuclear Station Unit-3 reactor vessel surveillance program. The objective of the program is to monitor the effects of neutron irradiation on the tensile and fracture toughness properties of the reactor vessel materials by the testing and evaluation of tension and Charpy impact specimen. The program was designed in accordance with the requirements of Appendix H to 10CFR50 and ASTM Specification E185-73.

The capsule received an average fast fluence of 1.45×10^{19} n/cm² (E > 1.0 MeV) and the predicted fast fluence for the reactor vessel T/4 location at the end of the eleventh cycle is 2.18×10^{18} n/cm² (E > 1 MeV). Based on the calculated fast flux at the vessel wall, an 80% capacity factor, and the planned fuel management, the projected peak fast fluence that the Oconee Unit-3 reactor pressure vessel inside surface will receive in 40 calendar years of operation is 9.49×10^{18} n/cm² (E > 1 MeV).

The results of the tension tests indicated that the materials exhibited normal behavior relative to neutron fluence exposure. The Charpy impact data results exhibited the characteristic behavior of shift to higher temperature for the 30 ft-lb transition temperature and a decrease in upper-shelf energy. These results demonstrated that the current techniques used for predicting the change in both the increase in the RT_{NDT} and the decrease in upper shelf properties due to irradiation are conservative.

The recommended operating period was extended to 15 effective full power years as a result of the third capsule evaluation. These new operating limitations are in accordance with the requirements of Appendix G of 10CFR50.

This revision corrects reactor vessel fluence values and eliminates the pressure-temperature operating limits for 21 and 24 EFPY.

RECORD OF REVISIONS

<u>Date</u>	<u>Revision Number</u>	<u>Description</u>
May 1991	0	Original Issue
May 1992	1	Summary - Revision statement added, fluence value revised Table 6-3 - Correct 21, 24, 32 EFPY fluence Table 7-5 - Corrected 32 EFPY data Table 7-6 - Corrected 32 EFPY data Section 8 - Deleted 21 and 24 EFPY pressure-temperature operating limit curves Section 9 - Fluence at EOL revised Section 11 - Revision signatures added Appendix D - Table D-2 fluence values corrected

CONTENTS

	Page
1. INTRODUCTION	1-1
2. BACKGROUND	2-1
3. SURVEILLANCE PROGRAM DESCRIPTION	3-1
4. PRE-IRRADIATION TESTS	4-1
4.1. Tension Tests	4-1
4.2. Impact Tests	4-1
5. POST-IRRADIATION TESTS	5-1
5.1. Thermal Monitors	5-1
5.2. Tension Test Results	5-1
5.3. Charpy V-Notch Impact Test Results	5-2
6. NEUTRON FLUENCE	6-1
6.1. Introduction	6-1
6.2. Vessel Fluence	6-4
6.3. Capsule Fluence	6-5
6.4. Fluence Uncertainties	6-5
7. DISCUSSION OF CAPSULE RESULTS	7-1
7.1. Pre-Irradiation Property Data	7-1
7.2. Irradiated Property Data	7-1
7.2.1. Tensile Properties	7-1
7.2.2. Impact Properties	7-2
7.3. Reactor Vessel Fracture Toughness	7-4
8. DETERMINATION OF REACTOR COOLANT PRESSURE BOUNDARY PRESSURE - TEMPERATURE LIMITS	8-1
9. SUMMARY OF RESULTS	9-1
10. SURVEILLANCE CAPSULE REMOVAL SCHEDULE	10-1
11. CERTIFICATION	11-1

Contents (Cont'd)

<u>APPENDIXES</u>	Page
A. Reactor Vessel Surveillance Program Background Data and Information	A-1
B. Pre-Irradiation Tensile Data	B-1
C. Pre-Irradiation Charpy Impact Data	C-1
D. Fluence Analysis Methodology	D-1
E. Capsule Dosimetry Data	E-1
F. References	F-1

List of Tables

Table

3-1. Specimens in Surveillance Capsule OCIII-D	3-3
3-2. Chemical Composition and Heat Treatment of Surveillance Materials	3-4
5-1. Tensile Properties of Capsule OCIII-D Base Metal and Weld Metal Irradiated to 1.45×10^{19} n/cm ² (E > 1 MeV)	5-3
5-2. Charpy Impact Data From Capsule OCIII-D Base Metal, ANK-191, Transverse Orientation, Irradiated to 1.45×10^{19} n/cm ² (E > 1 MeV);	5-3
5-3. Charpy Impact Data From Capsule OCIII-D, Base Metal, AWS-192, Transverse Orientation, Irradiated to 1.45×10^{19} n/cm ² (E > 1 MeV)	5-4
5-4. Charpy Impact Data From Capsule OCIII-D HAZ Metal, ANK-191, Longitudinal Orientation, Irradiated to 1.45×10^{19} n/cm ² (E > 1 MeV)	5-4
5-5. Charpy Impact Data From Capsule OCIII-D HAZ Metal, AWS-192, Longitudinal Orientation, Irradiated to 1.45×10^{19} n/cm ² (E > 1 MeV)	5-5
5-6. Charpy Impact Data From Capsule OCIII-D Weld Metal WF-209-1 Irradiated to 1.45×10^{19} n/cm ² (E > 1 MeV)	5-5
5-7. Charpy Impact Data From Capsule OCIII-D Correlation Monitor Material, Heat No. A-1195-1, Irradiated to 1.45×10^{19} n/cm ² (E > 1 MeV)	5-6
6-1. Surveillance Capsule Dosimeters	6-6
6-2. Oconee Unit-3 Reactor Vessel Fast Flux	6-7
6-3. Calculated Oconee Unit-3 Reactor Vessel Fluence	6-8
6-4. Surveillance Capsule OCIII-D Fluence, Flux, and DPA	6-9
6-5. Estimated Fluence Uncertainty	6-9
7-1. Comparison of Capsule OCIII-D Tensile Test Results	7-6
7-2. Summary of Oconee Unit 3 Reactor Vessel Surveillance Capsules Tensile Test Results	7-7
7-3. Observed Vs. Predicted Changes for Capsule OCIII-D Irradiated Charpy Impact Properties - 1.45×10^{19} n/cm ² (E > 1 MeV)	7-8

Tables (Cont'd)

Table	Page
7-4. Summary of Oconee Unit 3 Reactor Vessel Surveillance Capsules Charpy Impact Test Results	7-9
7-5. Evaluation of Reactor Vessel End-of-Life Fracture Toughness and Pressuriz Thermal Shock Criterion - Duke Power Company, Oconee Unit-3 (32 EFPY)	7-10
7-6. Evaluation of Duke Power Company Oconee Unit-3 Reactor Vessel End-of-Life, Upper Shelf Energy (32 EFPY)	7-11
8-1. Data for Preparation of Pressure-Temperature Limit Curves for Oconee Unit-3 -- Applicable Through 15 EFPY	8-4
A-1. Surveillance Program Material Selection Data for Oconee 3	A-3
A-2. Materials and Specimens in Upper Surveillance Capsules OCIII-A, OCIII-C, and OCIII-E	A-4
A-3. Materials and Specimens in Lower Surveillance Capsules OCIII-B, OCIII-D, and OCIII-F	A-4
B-1. Pre-Irradiation Tensile Properties of Shell Plate Material, Heat ANK-191	B-2
B-2. Pre-Irradiation Tensile Properties of Weld Metal - Longitudinal, WF-209-1	B-2
C-1. Pre-Irradiation Charpy Impact Data for Shell Forging Material - Transverse Orientation, Heat ANK-191	C-2
C-2. Pre-Irradiation Charpy Impact Data for Shell Forging Material - Transverse Orientation, Heat AWS-192	C-3
C-3. Pre-Irradiation Charpy Impact Data for Shell Forging Material - HAZ, Transverse Orientation, Heat ANK-191	C-4
C-4. Pre-Irradiation Charpy Impact Data for Shell Forging Material - HAZ, Transverse Orientation, Heat AWS-192	C-5
C-5. Pre-Irradiation Charpy Impact Data for Weld Metal, WF-209-1	C-6
D-1. Flux Normalization Factor	D-7
D-2. Oconee Unit 3 Reactor Vessel Fluence by Cycle	D-8
E-1. Detector Composition and Shielding	E-2
E-2. Measured Specific Activities (Unadjusted) for Dosimeters in Capsule OCIII-D	E-2
E-3. Dosimeter Activation Cross Sections, b/atom	E-3

List of Figures

Figure	
3-1. Reactor Vessel Cross Section Showing Location of Capsule OCIII-D Duke Power Company Oconee Unit-3	3-5
3-2. Reactor Vessel Cross Section Showing Location of Oconee Unit 3 Capsule OCIII-D in Crystal River Unit 3 Reactor	3-6
3-3. Loading Diagram for Test Specimens in Capsule OCIII-D	3-7
5-1. Charpy Impact Data for Irradiated Base Material, Transverse Orientation, Heat No. ANK-191	5-7

Figures (Cont'd)

Figure	Page
5-2. Charpy Impact Data for Irradiated Base Material, Transverse Orientation, Heat No. AWS-192	5-8
5-3. Charpy Impact Data for Irradiated Base Material, Heat-Affected Zone, Heat No. ANK-191	5-9
5-4. Charpy Impact Data for Irradiated Base Material, Heat-Affected Zone, Heat No. AWS-192	5-10
5-5. Charpy Impact Data for Irradiated Weld Metal, WF-209-1	5-11
5-6. Charpy Impact Data for Irradiated Correlation Material, Correlation Material, HSST PL-02, Heat No. A-1195-1	5-12
6-1. General Fluence Determination Methodology	6-2
6-2. Fast Flux, Fluence and DPA Distribution Through Reactor Vessel Wall	6-10
6-3. Azimuthal Flux and Fluence Distributions at Reactor Vessel Inside Surface	6-11
8-1. Predicted Fast Neutron Fluence at Various Locations Through Reactor Vessel Wall for 32 EFPY - Oconee Unit-3	8-5
8-2. Reactor Vessel Pressure-Temperature Limit Curves for Normal Operation - Heatup, Applicable for First 15 EFPY - Oconee Unit-3	8-6
8-3. Reactor Vessel Pressure-Temperature Limit Curves for Normal Operation - Cooldown, Applicable for First 15 EFPY - Oconee Unit-3	8-7
8-4. Reactor Vessel Pressure-Temperature Limit Curves for Inservice Leak and Hydrostatic Tests, Applicable for First 15 EFPY - Oconee Unit-3	8-8
A-1. Location and Identification of Materials Used in Fabrication of Reactor Pressure Vessel	A-5
C-1. Charpy Impact Data from Unirradiated Shell Forging Material (ANK-191), Transverse Orientation	C-7
C-2. Charpy Impact Data from Unirradiated Shell Forging Material (AWS-192), Transverse Orientation	C-8
C-3. Charpy Impact Data from Unirradiated Shell Forging Material (ANK-191), Heat-Affected Zone, Longitudinal Orientation	C-9
C-4. Charpy Impact Data from Unirradiated Shell Forging Material (AWS-192), Heat-Affected Zone, Longitudinal Orientation	C-10
C-5. Charpy Impact Data from Unirradiated Weld Metal WF-209-1	C-11
D-1. Rationale for the Calculation of Dosimeter Activities and Neutron Flux in the Capsule	D-9
D-2. Rationale for the Calculation of Neutron Flux in the Reactor Vessel	D-10
D-3. Plan View Through Reactor Core Midplane (Reference R-θ Calculation Model)	D-11

1. INTRODUCTION

This report describes the results of the examination of the third capsule (OCIII-D) of the Duke Power Company, Oconee Nuclear Station Unit-3 (Oconee Unit-3) reactor vessel material surveillance program (RVSP). The capsule was removed and evaluated after being irradiated in the Crystal River Unit 3 reactor as part of the Integrated Reactor Vessel Materials Surveillance Program (BAW-1543A). This irradiation in Crystal River Unit 3 plus the previous irradiation in Oconee Unit-3 is the equivalent of 22.22 years of exposure in the Oconee Unit-3 reactor vessel. The capsule experienced a fluence of 1.45×10^{19} n/cm² (E > 1 MeV), which is the equivalent to approximately 57 effective full power years' (EFPY) operation of the Oconee Unit-3 reactor vessel. The first capsule (OCIII-A) from this program was removed and examined after the first year of operation; the results are reported in BAW-1438.² The second capsule (OCIII-B) was removed and examined after irradiation in Florida Power Corporation Crystal River Unit-3 as part of the Integrated Reactor Vessel Materials Surveillance Program; the results are reported in BAW-1697.³

The objective of the program is to monitor the effects of neutron irradiation on the tensile and impact properties of reactor pressure vessel materials under actual operating conditions. The surveillance program for Oconee Unit-3 was designed and furnished by Babcock & Wilcox (B&W) as described in BAW-10006A⁴ and conducted in accordance with BAW-1543A.¹ The program was planned to monitor the effects of neutron irradiation on the reactor vessel materials for the 40-year design life of the reactor pressure vessel.

The surveillance program for Oconee Unit-3 was designed in accordance with E185-66⁵ and thus is not in compliance with 10CFR50, Appendixes G⁶ and H⁷ since the requirements did not exist at the time the program was design. Because of the difference, additional tests and evaluations were required to ensure meeting

the requirements of 10 CFR 50, Appendixes G and H. The recommendations for the future operation of Oconee Unit-3 included in this report do comply with these requirements.

2. BACKGROUND

The ability of the reactor pressure vessel to resist fracture is the primary factor in ensuring the safety of the primary system in light water-cooled reactors. The beltline region of the reactor vessel is the most critical region of the vessel because it is exposed to neutron irradiation. The general effects of fast neutron irradiation on the mechanical properties of such low-alloy ferritic steels as SA508, Class 2, modified by ASME Code Case 1332-4, used in the fabrication of the Oconee Unit-3 reactor vessel, are well characterized and documented in the literature. The low-alloy ferritic steels used in the beltline region of reactor vessels exhibit an increase in ultimate and yield strength properties with a corresponding decrease in ductility after irradiation. The most significant mechanical property change in reactor pressure vessel steels is the increase in temperature for the transition from brittle to ductile fracture accompanied by a reduction in the Charpy upper shelf energy value.

Appendix G to 10CFR50, "Fracture Toughness Requirements,"⁶ specifies minimum fracture toughness requirements for the ferritic materials of the pressure-retaining components of the reactor coolant pressure boundary (RCPB) of water-cooled power reactors, and provides specific guidelines for determining the pressure-temperature limitations on operation of the RCPB. The toughness and operational requirements are specified to provide adequate safety margins during any condition of normal operation, including anticipated operational occurrences and system hydrostatic tests, to which the pressure boundary may be subjected over its service lifetime. Although the requirements of Appendix G to 10CFR50 became effective on August 13, 1973, the requirements are applicable to all boiling and pressurized water-cooled nuclear power reactors, including those under construction or in operation on the effective date.

Appendix H to 10CFR50, "Reactor Vessel Materials Surveillance Program Requirements,"⁷ defines the material surveillance program required to monitor changes in the fracture toughness properties of ferritic materials in the reactor vessel beltline region of water-cooled reactors resulting from exposure to neutron irradiation and the thermal environment. Fracture toughness test data are obtained from material specimens withdrawn periodically from the reactor vessel. These data will permit determination of the conditions under which the vessel can be operated with adequate safety margins against fracture throughout its service life.

A method for guarding against brittle fracture in reactor pressure vessels is described in Appendix G to the ASME Boiler and Pressure Vessel Code, Section III, "Nuclear Power Plant Components."⁸ This method utilizes fracture mechanics concepts and the reference nil-ductility temperature, RT_{NDT} , which is defined as the greater of the drop weight nil-ductility transition temperature (per ASTM E-208) or the temperature that is 60F below that at which the material exhibits 50 ft-lbs and 35 mils lateral expansion. The RT_{NDT} of a given material is used to index that material to a reference stress intensity factor curve (K_{IR} curve), which appears in Appendix G of ASME Section III. The K_{IR} curve is a lower bound of dynamic, static, and crack arrest fracture toughness results obtained from several heats of pressure vessel steel. When a given material is indexed to the K_{IR} curve, allowable stress intensity factors can be obtained for this material as a function of temperature. Allowable operating limits can then be determined using these allowable stress intensity factors.

The RT_{NDT} and, in turn, the operating limits of a nuclear power plant, can be adjusted to account for the effects of radiation on the properties of the reactor vessel materials. The radiation embrittlement and the resultant changes in mechanical properties of a given pressure vessel steel can be monitored by a surveillance program in which a surveillance capsule containing prepared specimens of the reactor vessel materials is periodically removed from the operating nuclear reactor and the specimens are tested. The increase in the Charpy V-notch 30 ft-lb temperature is added to the original RT_{NDT} to adjust it for radiation embrittlement. This adjusted RT_{NDT} is used to index the material to the K_{IR} curve which, in turn, is used to set operating limits for the nuclear

power plant. These new limits take into account the effects of irradiation on the reactor vessel materials.

Appendix G, 10CFR50, also requires a minimum Charpy V-notch upper-shelf energy of 75 ft-lbs for all beltline region materials unless it is demonstrated that lower values of upper-shelf fracture energy will provide an adequate margin for deterioration as the result of neutron radiation. No action is required for a material that does not meet the 75 ft-lb requirement provided the irradiation deterioration does not cause the upper-shelf energy to drop below 50 ft-lbs. The regulations specify that if the upper-shelf energy drops below 50 ft-lbs it must be demonstrated in a manner approved by the Office of Nuclear Regulation that the lower values will provide adequate margins of safety.

When a reactor vessel fails to meet the 50 ft-lb requirement, a program must be submitted for review and approval at least three years prior to the time the predicted fracture toughness will no longer satisfy the regulatory requirements. The program must address the following:

- A. A volumetric examination of 100 percent of the beltline materials that do not meet the requirement.
- B. Supplemental fracture toughness data as evidence of the fracture toughness of the irradiated beltline materials.
- C. Fracture toughness analysis to demonstrate the existence of equivalent margins of safety for continued operation.

If these procedures do not indicate the existence of an adequate margin of safety, the reactor vessel beltline may be given a thermal annealing treatment to recover the fracture toughness properties of the materials.

3. SURVEILLANCE PROGRAM DESCRIPTION

The surveillance program for Oconee Unit-3 comprises six surveillance capsules designed to monitor the effects of neutron and thermal environment on the materials of the reactor pressure vessel core region. The capsules, which were inserted into the reactor vessel before initial plant startup, were positioned inside the reactor vessel between the thermal shield and the vessel wall at the locations shown in Figure 3-1. The six capsules, originally designed to be placed two in each holder tube, are positioned near the peak axial and azimuthal neutron flux. BSW-10006A includes a full description of the capsule locations and design. After the capsules were removed from Oconee Unit-3 in 1976 and included in the integrated RVSP, they were scheduled and irradiated in the Crystal River Unit 3 reactor as described in BAW-1543A. During this period of irradiation, capsule OCIII-D was irradiated in the bottom location in holder tube YX as shown in Figure 3-2.

Capsule OCIII-D was removed during the seventh refueling shutdown of Crystal River Unit 3. This capsule contained Charpy V-notch impact test specimens fabricated from one base metal (SA508, Class 2), one heat-affected-zone, a weld metal and correlation material. Tension test specimens were fabricated from the base metal and the weld metal only. The specimens contained in the capsule are described in Table 3-1, and the location of the individual specimens within the capsule are described in Figure 3-3. The chemical composition and heat treatment of the surveillance material in capsule OCIII-D are described in Table 3-2.

All test specimens were machined from the 1/4-thickness (1/4T) location of the plate material. Charpy V-notch and tension test specimens were cut from the surveillance material such that they were oriented with their longitudinal axes either parallel or perpendicular to the principal working direction.

Capsule OCIII-D contained dosimeter wires, described as follows:

<u>Dosimeter Wire</u>	<u>Shielding</u>
U-Al alloy	Cd-Ag alloy
Np-Al alloy	Cd-Ag alloy
Nickel	Cd-Ag alloy
0.66% Co-Al alloy	Cd
0.66% Co-Al alloy	None
Fe	None

Thermal monitors of low-melting alloys and metals were included in the capsule. The alloys and metals and their melting points were as follows:

<u>Alloy</u>	<u>Melting Point, F</u>
97% Pb, 5% Ag, 5% Sn	558
97.5% Pb, 2.5% Ag	580
97.5% Pb, 1.5% Ag, 1.0% Sn	588
Cadmium, 99.99+%	610
Lead, 99.99+%	621

Table 3-1. Specimens in Surveillance Capsule OCIII-D

<u>Material Description</u>	<u>No. of Specimens</u>	
	<u>Tensile</u>	<u>Charpy</u>
Weld metal, WF-209, longitudinal	2	12
Weld, HAZ		
Heat A - ANK-191, longitudinal	0	12
Heat B - AWS-192, longitudinal	0	6
Baseline material		
Heat A - ANK-191, transverse	2	12
Heat B - AWS-192, transverse	0	6
Correlation, HSST plate 02	0	6
Total per capsule	4	54

Table 3-2. Chemical Composition and Heat Treatment of Surveillance Materials

Element	Chemical Analysis			
	Heat ANK-191 ^(a)	Heat AWS-192 ^(a)	Weld Metal WF-209-1B ^(b)	Correlation Material HSST-02 (A-1195-1) ^(c)
C	0.24	0.21	0.08	0.23
Mn	0.72	0.58	1.63	1.39
P	0.014	0.011	0.017	0.013
S	0.012	0.015	0.012	0.013
Si	0.21	0.24	0.61	0.21
Ni	0.76	0.73	0.58	0.64
Cr	0.34	0.30	0.10	---
Mo	0.62	0.60	0.39	0.50
Cu	0.02	0.01	0.30	0.17

Heat No.	Heat Treatment		
	Temp., F	Time, h	Cooling
ANK-191 ^(a)	1620-1660	4.0	Water quench
	1570-1610	4.0	Water quench
	1230-1270	10.0	Water quench
	1100-1150	40.0	Furnace-cooled
AWS-192 ^(a)	1620-1660	4.0	Water quench
	1570-1610	4.0	Water quench
	1220-1250	10.0	Water quench
	1100-1150	40.0	Furnace-cooled
WF-209-1B ^(c)	1100-1150	30.0	Furnace-cooled
A-1195-1 ^(d,e)	1600±75	4.0	Water quench
	1225±25	4.0	Furnace-cooled
	1125±25	40.0	Furnace cooled

^(a)Per BAW-1820.

^(b)Per BAW-1500 and BAW-1820.

^(c)ORNL-4463.⁸

^(d)Per plate section identification card.

^(e)Normalized at 1675F ± 75F.

Figure 3-1. Reactor Vessel Cross Section Showing Location of Capsule OCIII-D Duke Power Company Oconee Unit-3

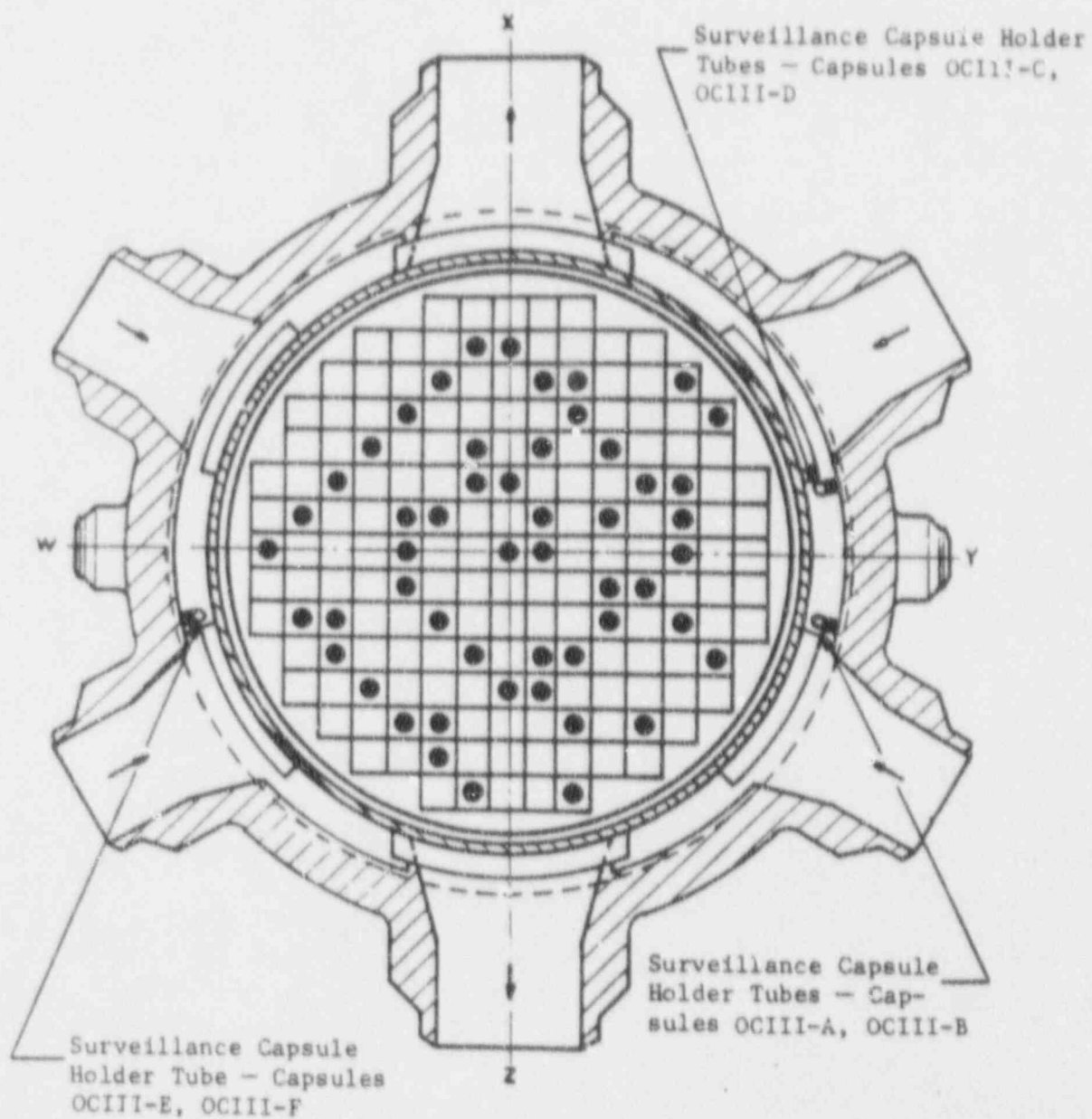


Figure 3-2. Reactor Vessel Cross Section Showing Location of Ocone Unit 3 Capsule OCIII-D in Crystal River Unit 3 Reactor

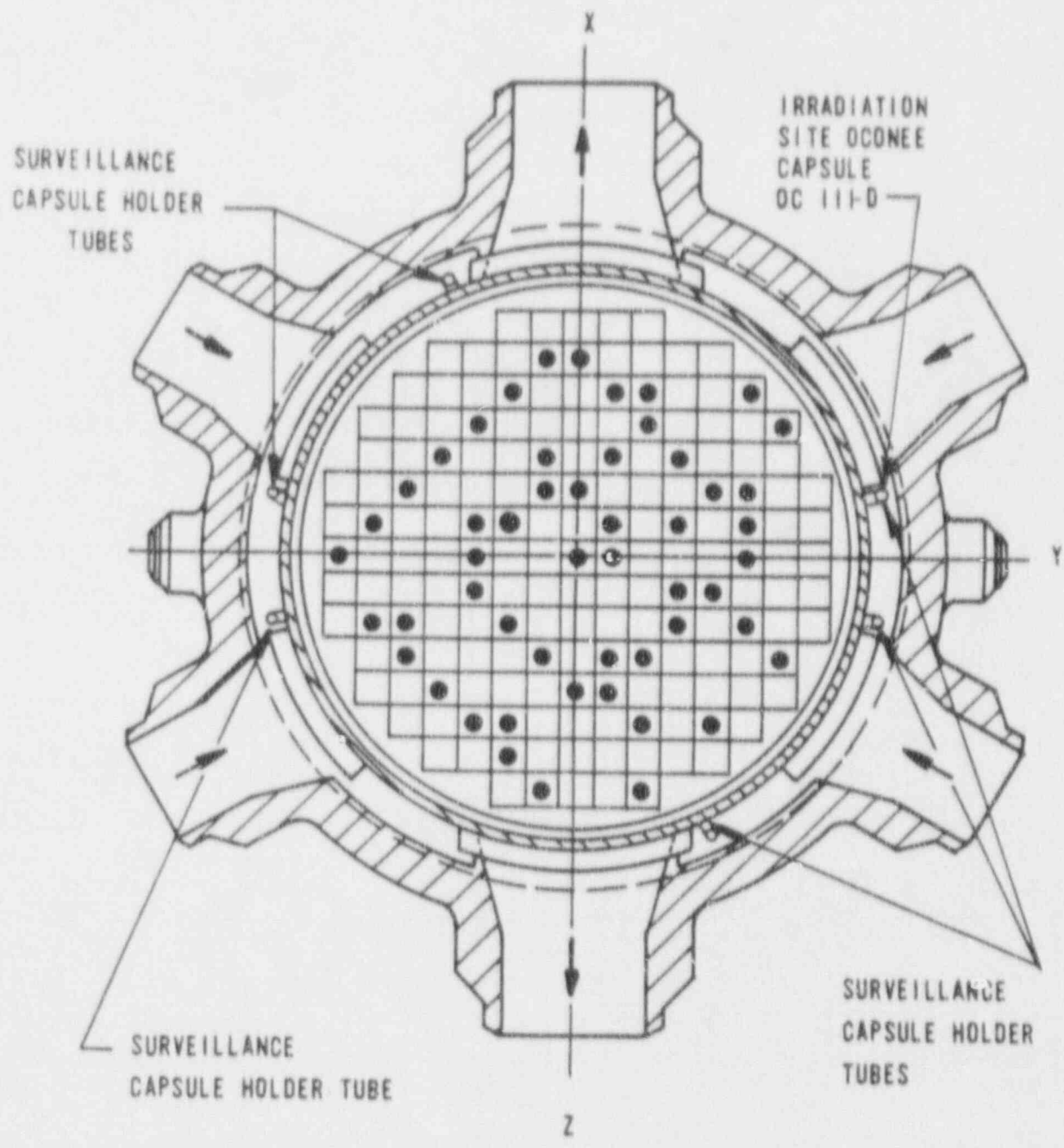
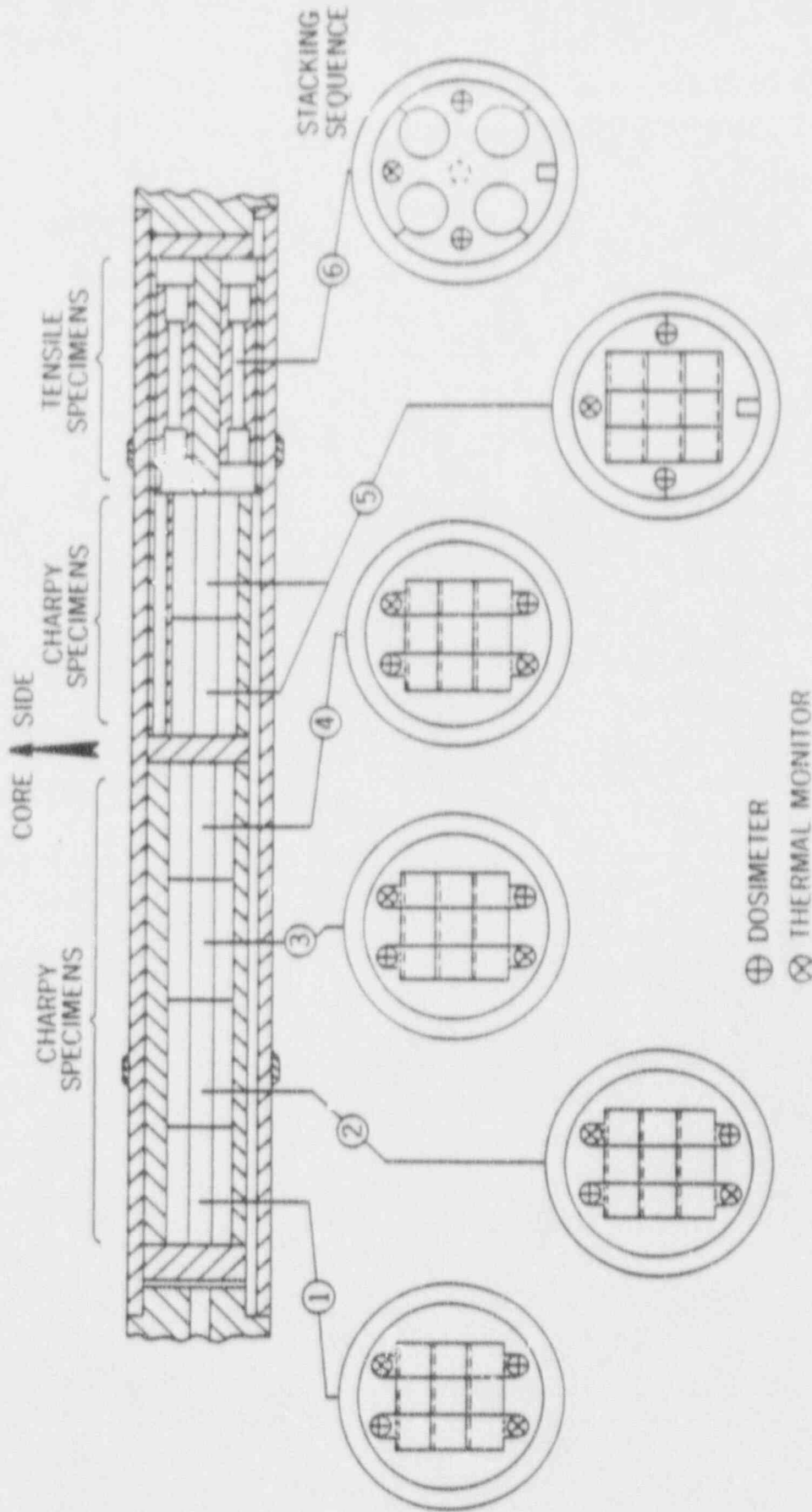


Figure 3-3. Loading Diagram for Test Specimens in Capsule OCIII-D



4. PRE-IRRADIATION TESTS

Unirradiated material was evaluated for two purposes: (1) to establish a baseline of data to which irradiated properties data could be referenced, and (2) to determine those materials properties to the extent practical from available material, as required for compliance with 10CFR50, Appendixes G and H.

4.1. Tension Tests

Tension test specimens were fabricated from the reactor vessel shell course forging and weld metal. The specimens were 4.25 inches long with a reduced section 1.750 inches long by 0.357 inch in diameter. They were tested on a 55,000-lb load capacity universal test machine at a crosshead speed of 0.050 inch per minute. A 4-pole extension device with a strain gaged extensometer was used to determine the 0.2% yield point. Test conditions were in accordance with the applicable requirements of ASTM A370-77.¹⁰ For each material type and/or condition, six specimens in groups of three were tested at both room temperature and 580F. The tension-compression load cell used had a certified accuracy of better than +0.5% of full scale (25,000 lb). All test data for the pre-irradiation tensile specimens are given in Appendix B.

4.2. Impact Tests

Charpy V-notch impact tests were conducted in accordance with the requirements of ASTM Standard Methods A370-77¹⁰ and E23-82¹¹ on an impact tester certified to meet Watertown standards. Test specimens were of the Charpy V-notch type, which were nominally 0.394 inch square and 2.165 inches long.

Prior to testing, specimens were temperature-controlled in liquid immersion baths, capable of covering the temperature range from -50 to +550F. Specimens were removed from the baths and positioned in the test frame anvil with tongs specifically designed for the purpose. The pendulum was released manually,

allowing the specimens to be broken within 5 seconds from their removal from the temperature baths.

Impact test data for the unirradiated baseline reference materials are presented in Appendix C. Tables C-1 through C-5 contain the basis data that are plotted in Figures C-1 through C-5.

5. POST-IRRADIATION TESTS

5.1. Thermal Monitors

Capsule OCIII-D contained two temperature monitor holder tubes, each containing five fusible alloy wires with melting points ranging from 558 to 621F. Four of the five wires in each set had the appearance of being melted. All the thermal monitors at 558, 580, and 588F had melted while those at the 610F location showed no signs of melting or slumping; the monitor at the 621F location appeared to be melted in both holder tubes. Heretofore it was assumed that the 610F and 621F monitors were placed in the wrong locations in the holder tubes, and based on these observations, it was concluded that the capsule had been exposed to a peak temperature in the range of 610 to 621F during the reactor operating period.

In the case of OCIII-D the original loading diagram was consulted. This drawing lists the five materials used in the monitors, and showed the position in which each wire was loaded. Both show the lead wire (621F melting point) to be in the fourth position, with the cadmium wire (610F melting point) in the fifth position. This means that the 610F monitor did not melt while the 621F monitor appeared to melt. It is believed that the lead wire softened and slumped and thereby presented the appearance of melting due to long exposure to elevated temperatures, which were not sufficient to melt the cadmium wire. Therefore, it is probable that the capsule was exposed to temperatures in excess of 588F but not as high as 610F, and that this was sufficient to cause the lead wires to slump and appear to have melted.

5.2. Tension Test Results

The results of the postirradiation tension tests are presented in Table 5-1. Tests were performed on specimens at both room temperature and at the temperature of 500F using similar test procedures and techniques used to test the unirradiated specimens (Section 4.1). In general, the ultimate strength and yield

strength of the material increased with a corresponding slight decrease in ductility as compared to the unirradiated values; both effects were the result of neutron radiation damage. The type of behavior observed and the degree to which the material properties changed is within the range of changes to be expected for the radiation environment to which the specimens were exposed.

The results of the pre-irradiation tension tests are presented in Appendix B.

5.3. Charpy V-Notch Impact Test Results

The test results from the irradiated Charpy V-notch specimens of the reactor vessel beltline material are presented in Tables 5-2 through 5-7 and Figures 5-1 through 5-6. The test procedures and techniques were similar to those used to test the unirradiated specimens (Section 4.2). The data show that the materials exhibited a sensitivity to irradiation within the values to be expected from their chemical composition and the fluence to which they were exposed.

The results of the pre-irradiation Charpy V-notch impact tests are given in Appendix C.

Table 5-1. Tensile Properties of Capsule OCIII-D Base Metal and Weld Metal Irradiated to 1.45×10^{19} n/cm² (E > 1 MeV)

Specimen No.	Test Temp., F	Strength, psi		Elongation, %		Red'n. in Area, %
		Yield	Ultimate	Uniform	Total	
<u>Base Metal, Transverse, Heat ANK-191</u>						
JJ 602	70	66,900	91,500	9.9	26.6	65.1
JJ 618	550	60,300	87,200	9.9	23.3	62.0
<u>Weld Metal, WF-209-1</u>						
JJ 017	70	98,000	111,300	10.7	24.2	56.7
JJ 016	550	86,600	102,900	9.0	17.7	49.4

Table 5-2. Charpy Impact Data From Capsule OCIII-D, Base Metal, ANK 191, Transverse Orientation, Irradiated to 1.45×10^{19} n/cm² (E > 1 MeV)

Specimen No.	Test Temp., F	Absorbed Energy, ft-lb	Lateral Expansion, 10 ⁻³ in.	Shear Fracture, %
JJ 634	0	9.0	02	10
JJ 693	25	23.0	23	10
JJ 646	30	39.0	30	10
JJ 683	30	63.0	50	20
JJ 659	40	58.0	51	20
JJ 669	70	71.5	57	30
JJ 624	125	107.0	76	70
JJ 677	200	123.0*	83	100
JJ 627	250	124.0*	99	100
JJ 615	350	128.5*	89	100
JJ 628	450	123.0	86	100
JJ 662	550	123.5	91	100

*Values used to determine upper-shelf energy value per ASTM E185.

Table 5-3. Charpy Impact Data From Capsule OCIII-D, Base Metal, AWS 192
Transverse Orientation, Irradiated to 1.45×10^{19} n/cm² (E > 1 MeV)

Specimen No.	Test Temp., F	Absorbed Energy, ft-lb	Lateral Expansion, 10 ⁻³ in.	Shear Fracture, %
KK 668	0	5.0	03	0
KK 615	40	37.0	29	10
KK 649	70	50.5	43	20
KK 660	125	84.0	64	60
KK 617	200	90.0	67	90
KK 638	300	93.0*	77	100

*Value used to determine upper-shelf energy value per ASTM E185.

Table 5-4. Charpy Impact Data From Capsule OCIII-D HAZ Metal, ANK 191
Longitudinal Orientation, Irradiated to 1.45×10^{19} n/cm² (E > 1 MeV)

Specimen No.	Test Temp., F	Absorbed Energy, ft-lb	Lateral Expansion, 10 ⁻³ in.	Shear Fracture, %
JJ 366	-50	23.5	13	10
JJ 349	0	25.0	16	20
JJ 329	25	31.5	20	30
JJ 326	70	136.5	90	90
JJ 361	70	26.5	30	20
JJ 378	70	138.0	97	100
JJ 367	100	63.0	40	50
JJ 360	125	62.0	46	85
JJ 307	200	75.0*	51	100
JJ 368	250	64.0*	51	100
JJ 356	350	66.0*	48	100
JJ 352	550	73.5	59	100

*Values used to determine upper-shelf energy value per ASTM E185.

Table 5-5. Charpy Impact Data From Capsule OCIII-D HAZ Metal, AWS-192
 Longitudinal Orientation, Irradiated to 1.45×10^{19} n/cm² (E > 1 MeV)

Specimen No.	Test Temp., F	Absorbed Energy, ft-lb	Lateral Expansion, 10 ⁻³ in.	Shear Fracture, %
KK 328	-50	36.0	22	10
KK 314	0	79.5	50	40
KK 311	70	115.0	78	100
KK 331	125	64.0	51	60
KK 329	200	75.0*	50	100
KK 322	300	108.0*	80	100

*Values used to determine upper-shelf energy value per ASTM E185.

Table 5-6. Charpy Impact Data From Capsule OCIII-D Weld Metal WF-209-1
 Irradiated to 1.45×10^{19} n/cm² (E > 1 MeV)

Specimen No.	Test Temp., F	Absorbed Energy, ft-lb	Lateral Expansion, 10 ⁻³ in.	Shear Fracture, %
JJ 037	70	18.0	18	20
JJ 011	125	16.5	16	10
JJ 045	160	30.0	27	40
JJ 058	175	27.0	31	70
JJ 051	185	22.0	19	30
JJ 052	200	41.0	38	90
JJ 044	250	49.5*	47	100
JJ 025	300	39.0*	36	100
JJ 021	350	39.5*	41	100
JJ 035	400	40.0*	40	100
JJ 012	450	47.0	47	100
JJ 005	550	39.0	45	100

*Values used to determine upper-shelf energy value per ASTM E185.

Table 5-7. Charpy Impact Data From Capsule OCIII-D Correlation Monitor Material, Heat No. A-1195-1, Irradiated to 1.45×10^{19} n/cm² (E > 1 MeV)

Specimen No.	Test Temp., F	Absorbed Energy, ft-lb	Lateral Expansion, 10 ⁻³ in.	Shear Fracture, %
JJ 907	70	14.0	11	10
JJ 904	125	27.0	22	20
JJ 906	175	31.0	29	30
JJ 912	250	79.0	66	70
JJ 913	300	97.5	77	90
JJ 909	375	91.0*	82	100

*Value used to determine upper-shelf energy value per ASTM E185.

Figure 5-1. Charpy Impact Data for Irradiated Base Material, Transverse Orientation, Heat No. ANK-191

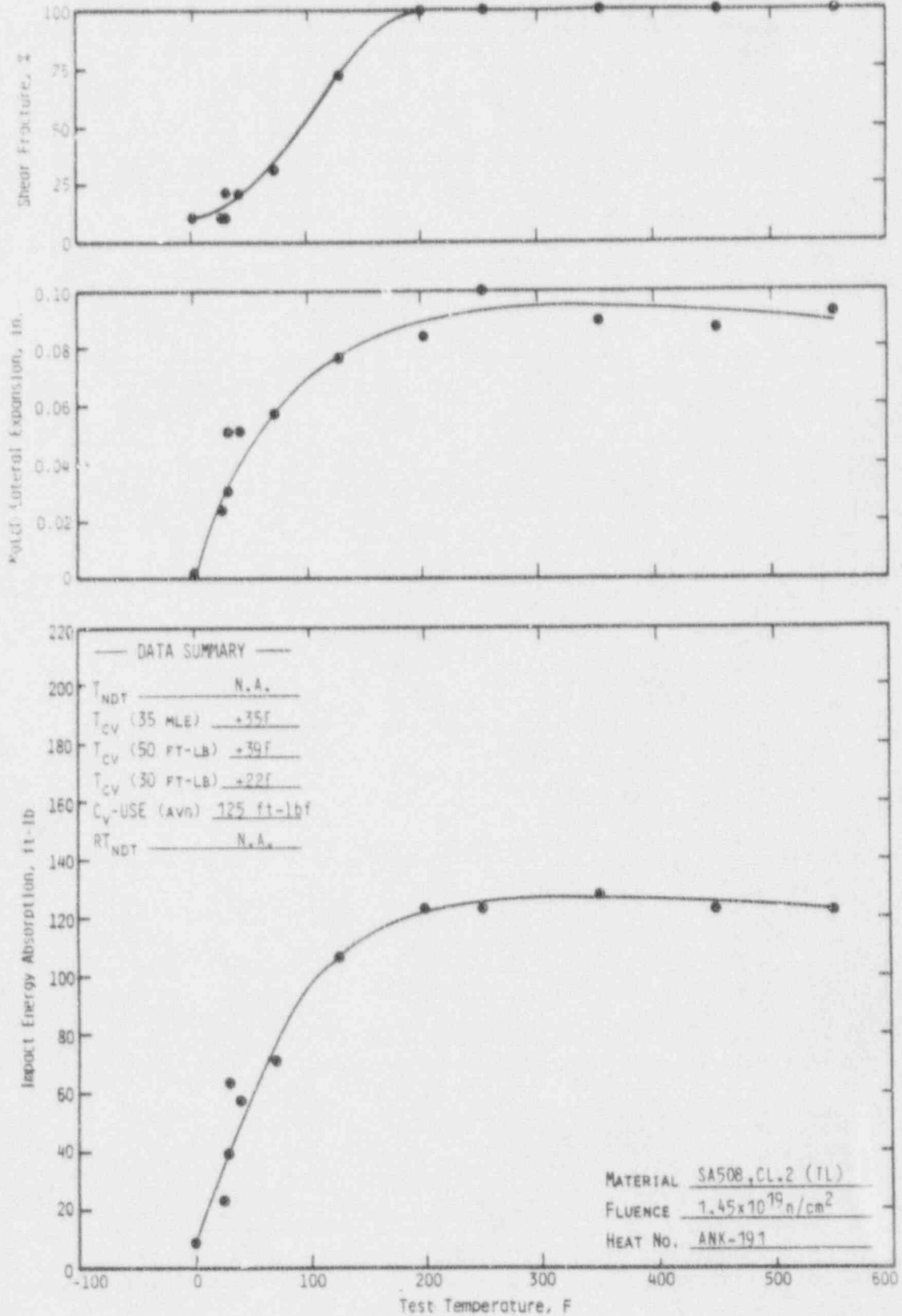


Figure 5-2. Charpy Impact Data for Irradiated Base Material, Transverse Orientation, Heat No. AWS-192

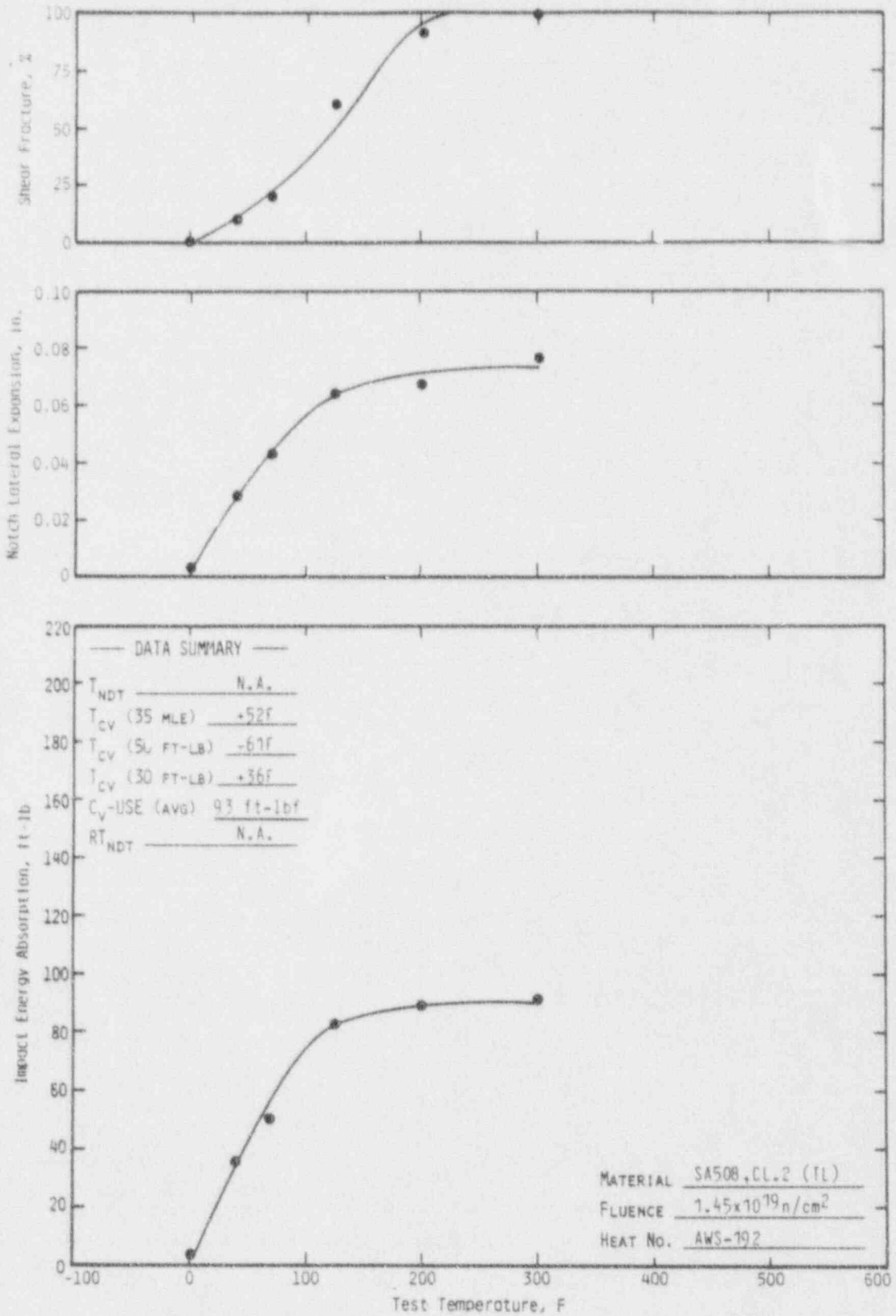


Figure 5-3. Charpy Impact Data for Irradiated Base Material.
Heat-Affected Zone, Heat No. ANK-191

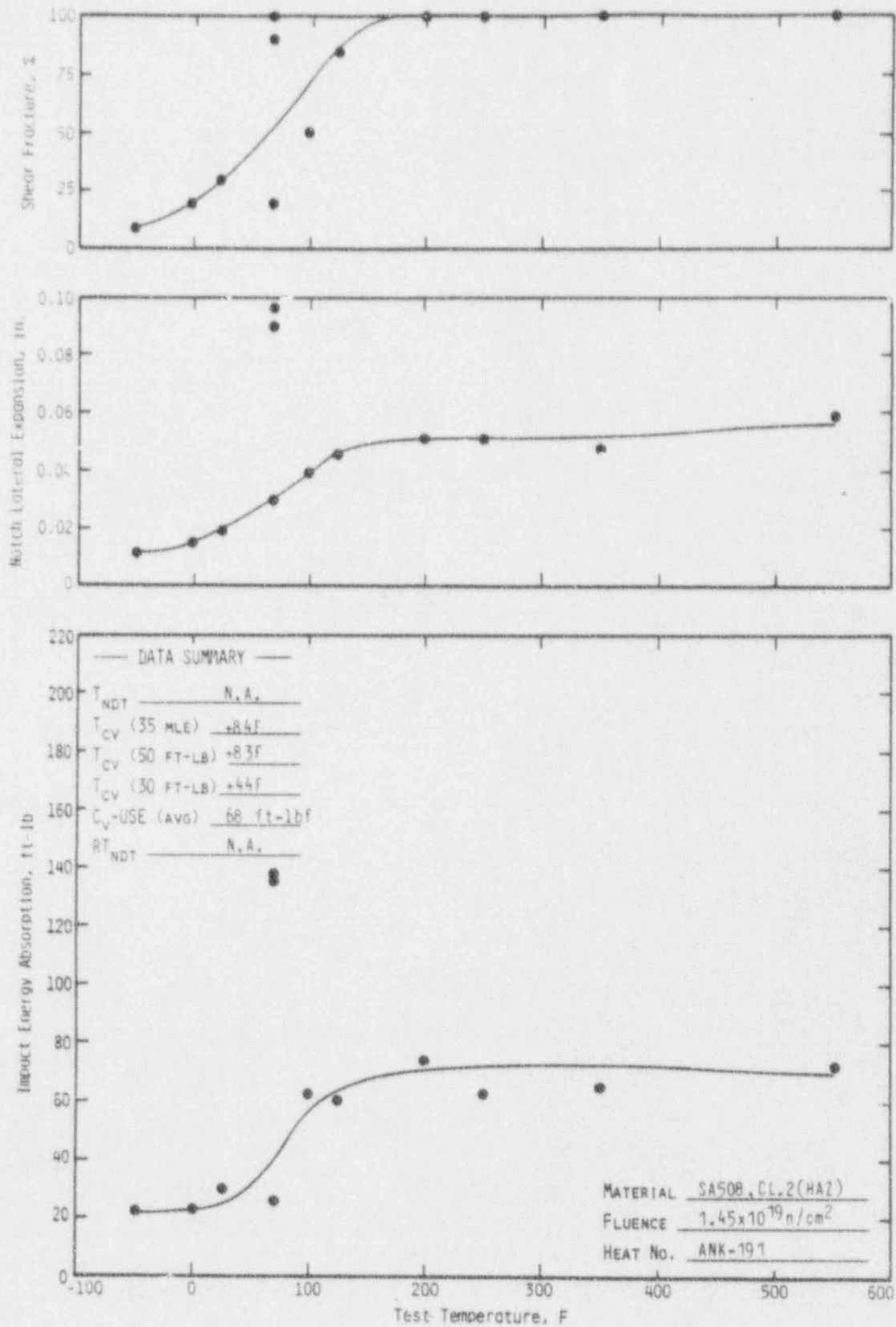


Figure 5-4. Charpy Impact Data for Irradiated Base Material, Heat-Affected Zone, Heat No. AWS-192

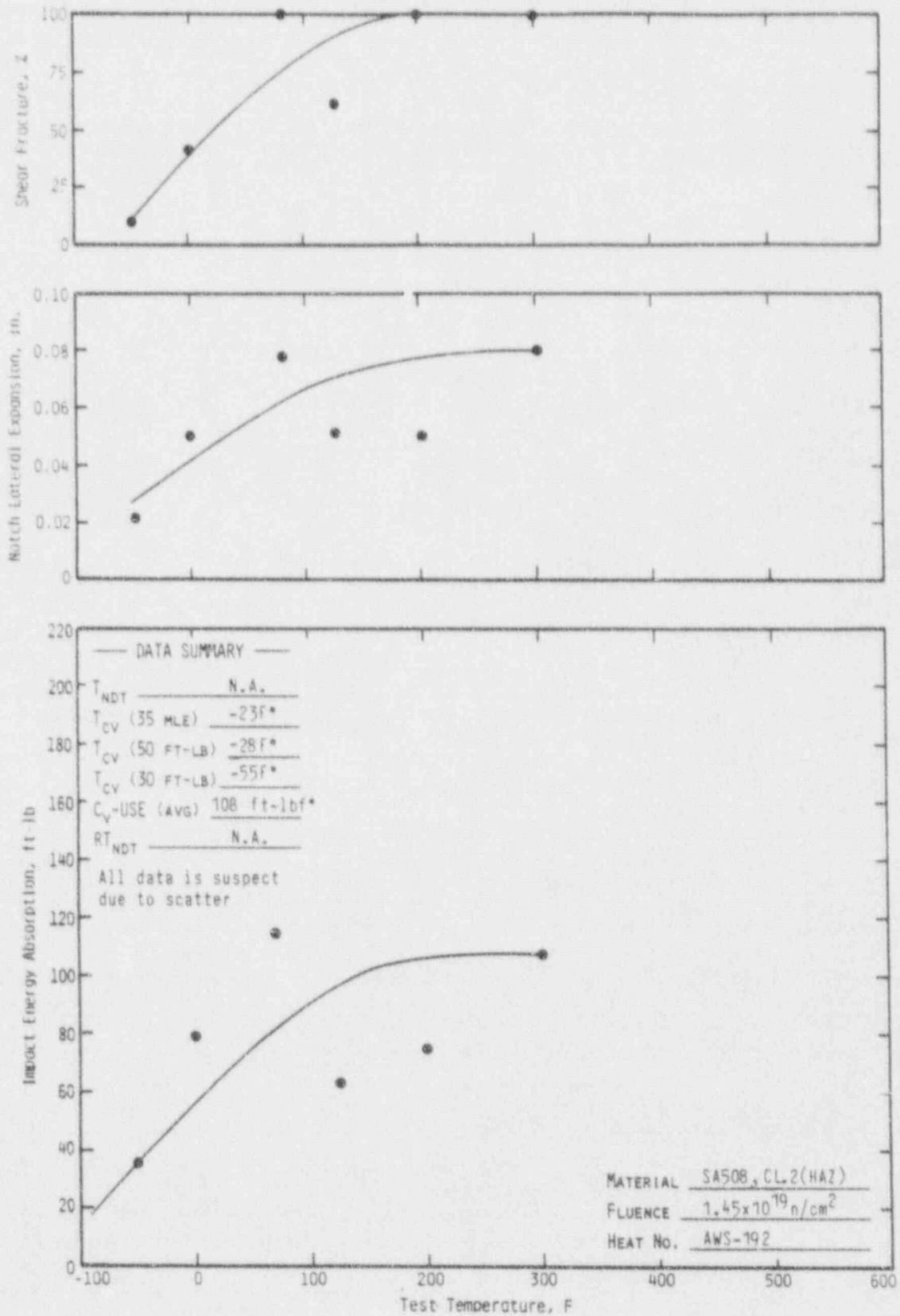


Figure 5-5. Charpy Impact Data for Irradiated Weld Metal, WF-209-1

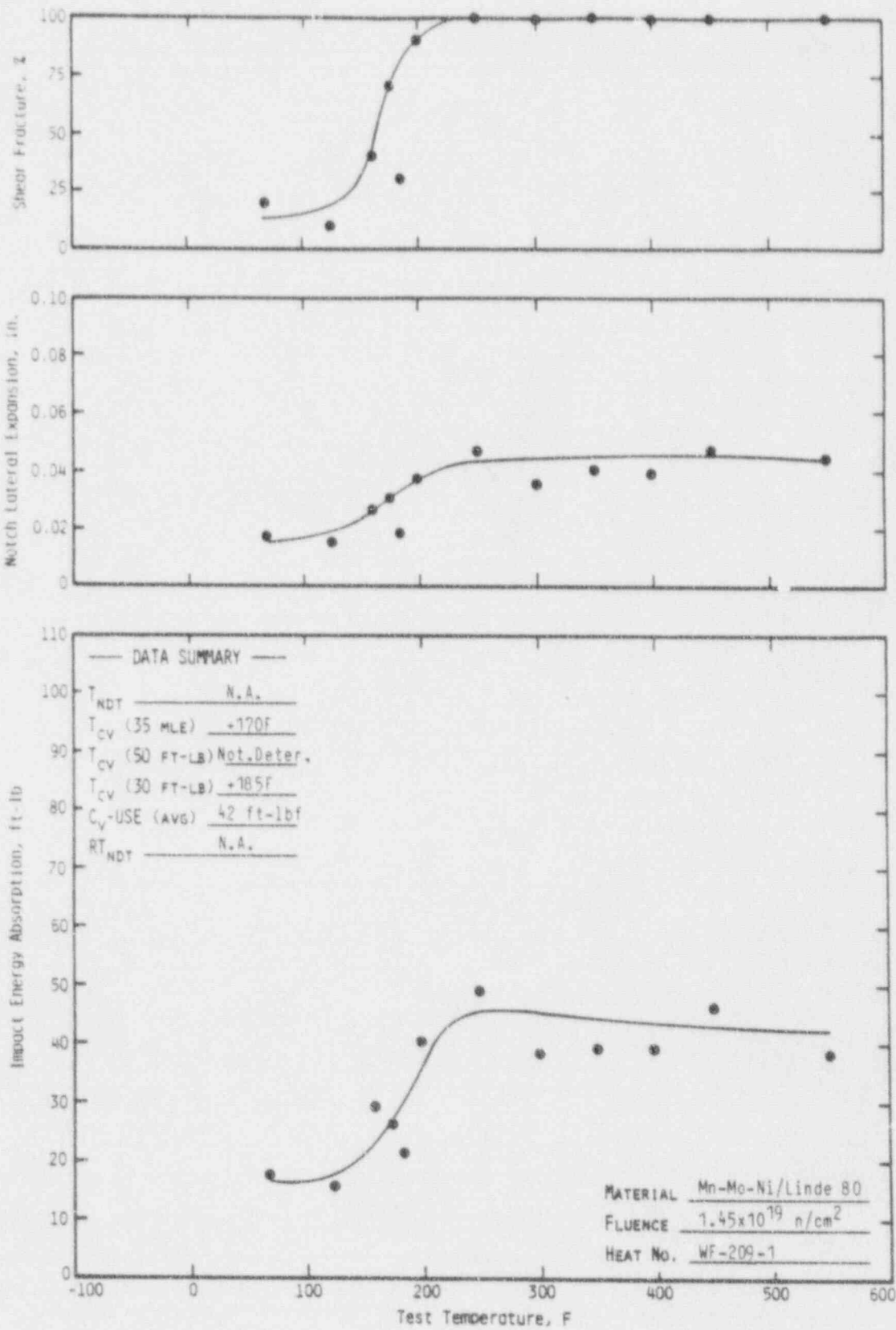
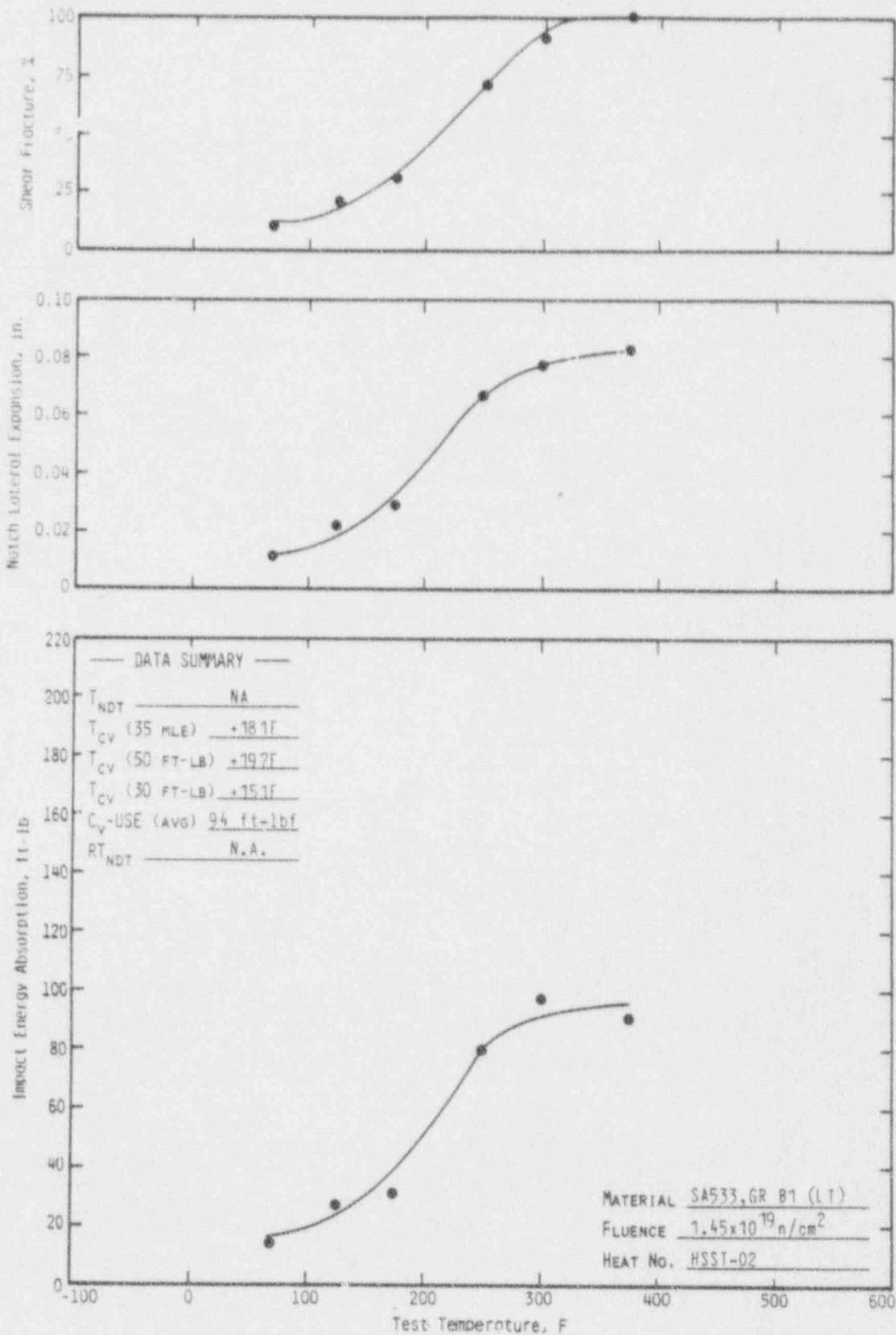


Figure 5-6. Charpy Impact Data for Irradiated Correlation Material, HSST PL-02, Heat No. A-1195-1



6. NEUTRON FLUENCE

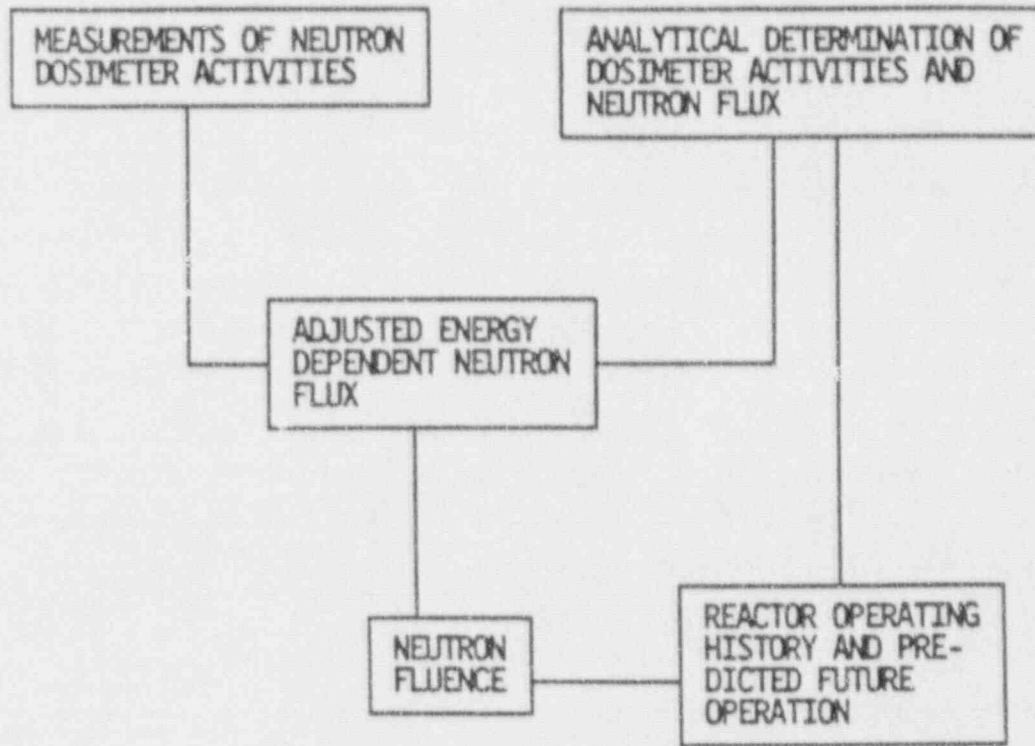
6.1. Introduction

The neutron fluence (time integral of flux) is a quantitative way of expressing the cumulative exposure of a material to a pervading neutron flux over a specific period of time. Fast neutron fluence, defined as the fluence of neutrons having energies greater than 1 MeV, is the parameter that is presently used to correlate radiation induced changes in material properties. Accordingly, the fast fluence must be determined at two locations: (1) in the test specimens located in the surveillance capsule, and (2) in the wall of the reactor vessel. The former is used in developing the correlation between fast fluence and changes in the material properties of specimens, and the latter is used to ascertain the point of maximum fluence in the reactor vessel, the relative radial and azimuthal distribution of the fluence, the fluence gradient through the reactor vessel wall, and the corresponding material properties.

The accurate determination of neutron flux is best accomplished through the simultaneous consideration of neutron dosimeter measurements and analytically derived flux spectra. Dosimeter measurements alone cannot be used to predict the fast fluence in the vessel wall or in the test specimens because (1) they cannot measure the fluence at the points of interest, and (2) they provide only rudimentary information about the neutron energy spectrum. Conversely, reliance on calculations alone to predict fast fluence is not prudent because of the length and complexity of the analytical procedures involved. In short, measurements and calculations are necessary complements of each other and together they provide assurance of accurate results.

Therefore, the determination of the fluence is accomplished using a combined analytical-empirical methodology which is outlined in Figure 6-1 and described in the following paragraphs. The details of the procedures and methods are presented in general terms in Appendix D and in BAW-1485P.¹²

Figure 6-1. General Fluence Determination Methodology



Analytical Determination of Dosimeter Activities and Neutron Flux

The analytical calculation of the space and energy dependent neutron flux in the test specimens and in the reactor vessel is performed with the two dimensional discrete ordinates transport code, DOTIV.¹³ The calculations employ an angular quadrature of 48 sectors (S8), a third order Legendre polynomial scattering approximation (P3), the CASK23E cross section set¹⁴ with 22 neutron energy groups and a fixed distributed source corresponding to the time weighted average power distribution for the applicable irradiation period.

In addition to the flux in the test specimens, the DOTIV calculation determines the saturated specific activity of the various neutron dosimeters located in the surveillance capsule using the ENDF/B5 dosimeter reaction cross sections.¹⁵ The saturated activity of each dosimeter is then adjusted by a factor which corrects for the fraction of saturation attained during the dosimeter's actual (finite)

irradiation history. Additional corrections are made to account for the following effects:

- Photon induced fissions in U and Np dosimeters (without this correction the results underestimate the measured activity).
- Fissile impurities in U dosimeters (without this correction the results underestimate the measured activity).
- Short half-life of isotopes produced in iron and nickel dosimeters (303-day Mn-54 and 71-day Co-58, respectively). (Without this correction, the results could be biased high or low depending on the long term versus short term power histories.)

Measurement of Neutron Dosimeter Activities

The accuracy of neutron fluence predictions is improved if the calculated neutron flux is compared with neutron dosimeter measurements adjusted for the effects noted above. The neutron dosimeters located in the surveillance capsules are listed in Table 6-1. Both activation type and fission type dosimeters were used.

The ratio of measured dosimeter activity to calculated dosimeter activity (M/C) is determined for each dosimeter, as discussed in Appendix D. These M/C ratios are evaluated on a case-by-case basis to assess the dependability or veracity of each individual dosimeter response. After carefully evaluating all factors known to affect the calculations or the measurements, an average M/C ratio is calculated and defined as the "normalization factor." The normalization factor is applied as an adjustment factor to the DOi-calculated flux at all points of interest.

Neutron Fluence

The determination of the neutron fluence from the time averaged flux requires only a simple multiplication by the time in EFPS (effective full-power seconds) over which the flux was averaged, i.e.

$$f_{ij}(\Delta T) = \sum_g \phi_{ig} \Delta T$$

where

$$f_{ij}(\Delta T) = \text{Fluence at } (i,j) \text{ accumulated over time } \Delta T \text{ (n/cm}^2\text{)},$$

g = Energy group index,

ϕ_{ijg} = Time-average flux at (i,j) in energy group g , (n/cm^2 -sec),

ΔT = Irradiation time, EFPS.

Neutron fluence was calculated in this analysis for the following components over the indicated operating time:

Test Specimens: Capsule irradiation time in EFPS

Reactor Vessel: Vessel irradiation time in EFPS

Reactor Vessel: Maximum point on inside surface extrapolated to 32 effective full power years

The neutron exposure to the reactor vessel and the material surveillance specimens was also determined in terms of the iron atom displacements per atom of iron (DPA). The iron DPA is an exposure index giving the fraction of iron atoms in an iron specimen which would be displaced during an irradiation. It is considered to be an appropriate damage exposure index since displacements of atoms from their normal lattice sites is a primary source of neutron radiation damage. DPA was calculated based on the ASTM Standard E693-79 (reapproved 1985).¹⁶ A DPA cross section for iron is given in the ASTM Standard in 641 energy groups. DPA per second is determined by multiplying the cross section at a given energy by the neutron flux at that energy and integrating over energy. DPA is then the integral of DPA per second over the time of the irradiation. In the DPA calculations reported herein, the ASTM DPA cross sections were first collapsed to the 22 neutron group structure of CASK-23E; the DPA was then determined by summing the group flux times the DPA cross section over the 22 energy groups and multiplying by the time of the irradiation.

6.2. Vessel Fluence

The maximum fluence ($E > 1$ MeV) exposure of the Oconee Unit 3 reactor vessel during Cycles 6-11 was determined to be 1.96×10^{18} n/cm^2 based on a maximum neutron flux of 9.49×10^9 n/cm^2 -s (Tables 6-2 and 6-3). The maximum fluence occurs at the cladding/vessel interface at an azimuthal location of approximately 11 degrees from a major horizontal axis of the core.

Fluence data were extrapolated to 32 EFPY of operation based on two assumptions: (1) the future fuel cycle operations do not differ significantly from their current designs, and (2) the latest calculated (or extrapolated) flux remains constant from that time through 32 EFPY. The extrapolation was carried out in two stages, (1) from EOC 11 to EOC 13, and (2) from EOC 13 to 32 EFPY. In the first stage, cycle averaged fluxes are calculated based on the current designs for cycle 12 and 13, using DOT adjoint factors for assembly-averaged power distributions. In the second stage, the 32 EFPY fluence was calculated by assuming a constant flux over the period which was equal to the average flux for cycles 12 and 13.

Relative fluence and DPA (displacement per atom) as a function of radial location in the reactor vessel wall is shown in Figure 6-2. Reactor vessel neutron fluence lead factors, which are the ratio of the neutron flux at the clad interface to that in the vessel wall at the T/4, T/2 and 3T/4 locations, are 1.78, 3.53, and 7.25, respectively. DPA lead factors at the same locations are 1.59, 2.64, and 4.55, respectively. The relative fluence as a function of azimuthal angle is shown in Figure 6-3. A peak occurs in the fast flux ($E > 1$ MeV) at about 11 degrees with a corresponding value of 9.49×10^8 n/cm²-s.

6.3. Capsule Fluence

The capsule was irradiated for 2373.9 EFPD in the top holder tube position during cycles 1B-7 of Crystal River Unit 3 located 11 degrees off the major horizontal axis at about 202 cm from the vertical axis of the core. The capsule was also irradiated for 477.9 EFPD in Oconee Unit 3, during cycle 1, located at the 11 degree position about 211 cm from the vertical axis of the core. The cumulative fast fluence at the center of the surveillance capsule was calculated to be 1.45×10^{18} n/cm² of which 5.1% was accumulated during the Oconee cycle 1 irradiation, and 94.9% was accumulated during the Crystal River cycles 1B-7 irradiation (Table 6-4). This fluence value represents an average value for the various locations in the capsule.

6.4. Fluence Uncertainties

Uncertainties were estimated for the fluence values reported herein. The results are shown in Table 6-5 and are based on comparisons to benchmark experiments,

when available; estimated and measured variations in input data; and on engineering judgement. The values in Table 6-5 represent best estimate values based on past experience with reactor vessel fluence analyses.

Table 6-1. Surveillance Capsule Dosimeters

<u>Dosimeter Reactions^(a)</u>	<u>Lower Energy Limit for Reaction, MeV</u>	<u>Isotope Half-Life</u>
$^{54}\text{Fe}(n,p)^{54}\text{Mn}$	2.5	312.5 days
$^{58}\text{Ni}(n,p)^{58}\text{Co}$	2.3	70.85 days
$^{238}\text{U}(n,f)^{137}\text{Cs}$	1.1	30.03 years
$^{237}\text{Np}(n,f)^{137}\text{Cs}$	0.5	30.03 years

(a) Reaction activities measured for capsule flux evaluation.

Table 6-2. Oconee Unit 3 Reactor Vessel Fast Flux

<u>Cycle</u>	<u>Fast Flux (E > 1 MeV), n/cm²-s</u>			<u>Flux n/cm²-s (E > 0.1 MeV) Inside Surface (Max Location)</u>
	<u>Inside Surface (Max Location)</u>	<u>T/4</u>	<u>3T/4</u>	
Cycle 1 (477.9 EFPD)	1.39E+10	7.73E+9	1.85E+9	2.78E+10
Cycles 2-5 (1020.1 EFPD)	1.55E+10	8.61E+9	1.96E+9	3.30E+10
Cycles 6-11 (2395.9 EFPD)	9.49E+9	5.32E+9	1.31E+9	1.99E+10
Cycle 12** (410 EFPD)	8.92E+9	5.07E+9*	1.23E+9*	----
Cycle 13** (410 EFPD)	7.62E+9	4.28E+9*	1.05E+9*	----
15 EFPY	8.27E+9	4.65E+9*	1.14E+9*	----
21 EFPY	8.27E+9	4.65E+9*	1.14E+9*	----
24 EFPY	8.27E+9	4.65E+9*	1.14E+9*	----
32 EFPY	8.27E+9	4.65E+9*	1.14E+9*	----

*Divide flux at inside surface by the appropriate lead factors on page 6-8 to obtain these T/4 and 3T/4 fast flux values.

**Assumed cycle length of 410 EFPD for flux extrapolation for Cycles 12 and 13.

Table 6-3. Calculated Oconee Unit 3 Reactor Vessel Fluence

Cumulative Irradiation Time	Fast Fluence, n/cm ² (E > 1 MeV)			
	Inside Surface (Max Location)	T/4	T/2	3T/4
End of Cycle 1 (477.9 EFPD)	0.58E+18	3.19E+17	7.73E+16	7.65E+16
End of Cycle 5 (1498 EFPD)	1.94E+18	1.05E+18	5.16E+17	2.50E+17
End of Cycle 11 (3893.9 EFPD)	3.91E+18	2.18E+18	1.17E+18	5.21E+17
End of Cycle 12 (4303.9 EFPD)	4.23E+18	2.38E+18*	1.20E+18*	5.83E+17*
End of Cycle 13 (4713.9 EFPD)	4.50E+18	2.53E+18*	1.27E+18*	6.21E+17*
15 EFPY	5.05E+18	2.84E+18*	1.43E+18*	6.97E+17*
21 EFPY	6.62E+18	3.72E+18*	1.88E+18*	9.13E+17*
24 EFPY	7.40E+18	4.16E+18*	2.10E+18*	1.02E+18*
32 EFPY	9.49E+18	5.33E+18*	2.69E+18*	1.31E+18*
*Calculated using these lead factors	1.0	1.78	3.53	7.25
<u>Conversion Factors</u>				
Fluence (E > 1 MeV) to DPA	1.45E-21**	1.63E-21**	1.94E-21**	2.31E-21**

**Multiply fast fluence values (E > 1 MeV) in units of n/cm² by these factors to obtain the corresponding DPA values.

Table 6-4. Surveillance Capsule OCIII-D Fluence, Flux, and DPA

<u>Irradiation Time</u>	<u>Flux (E > 1 MeV), n/cm²-s</u>	<u>Fluence, n/cm²</u>	<u>DPA</u>
OC3, Cycle 1 (477.9 EFPD)	2.48E+10	7.39E+17	1.41E-3
CR3, Cycle 1B-7, (2373.9 EFPD)	6.65E+10	1.38E+19	1.90E-2
Total	---	1.45E+19	2.05E-2

Table 6-5. Estimated Fluence Uncertainty

<u>Calculated Fluence</u>	<u>Estimated Uncertainty</u>	<u>Basis of Estimate</u>
In the capsule	± 15%	Activity measurements, cross section fission yields, saturation factor, deviation from average fluence value
In the reactor vessel at maximum location for cycles 1 through 11 of Oconee Unit 3	± 21%	Activity measurements, cross sections, fission yields, factors, axial factor, capsule location, radial/azimuthal extrapolation, normalization factor
In the reactor vessel at the maximum location for end-of-life extrapolation	± 23%	Factors in vessel fluence above plus uncertainties for extrapolation to 32 EFPY

Figure 6-2. Fast Flux, Fluence and DPA Distribution Through Reactor Vessel Wall

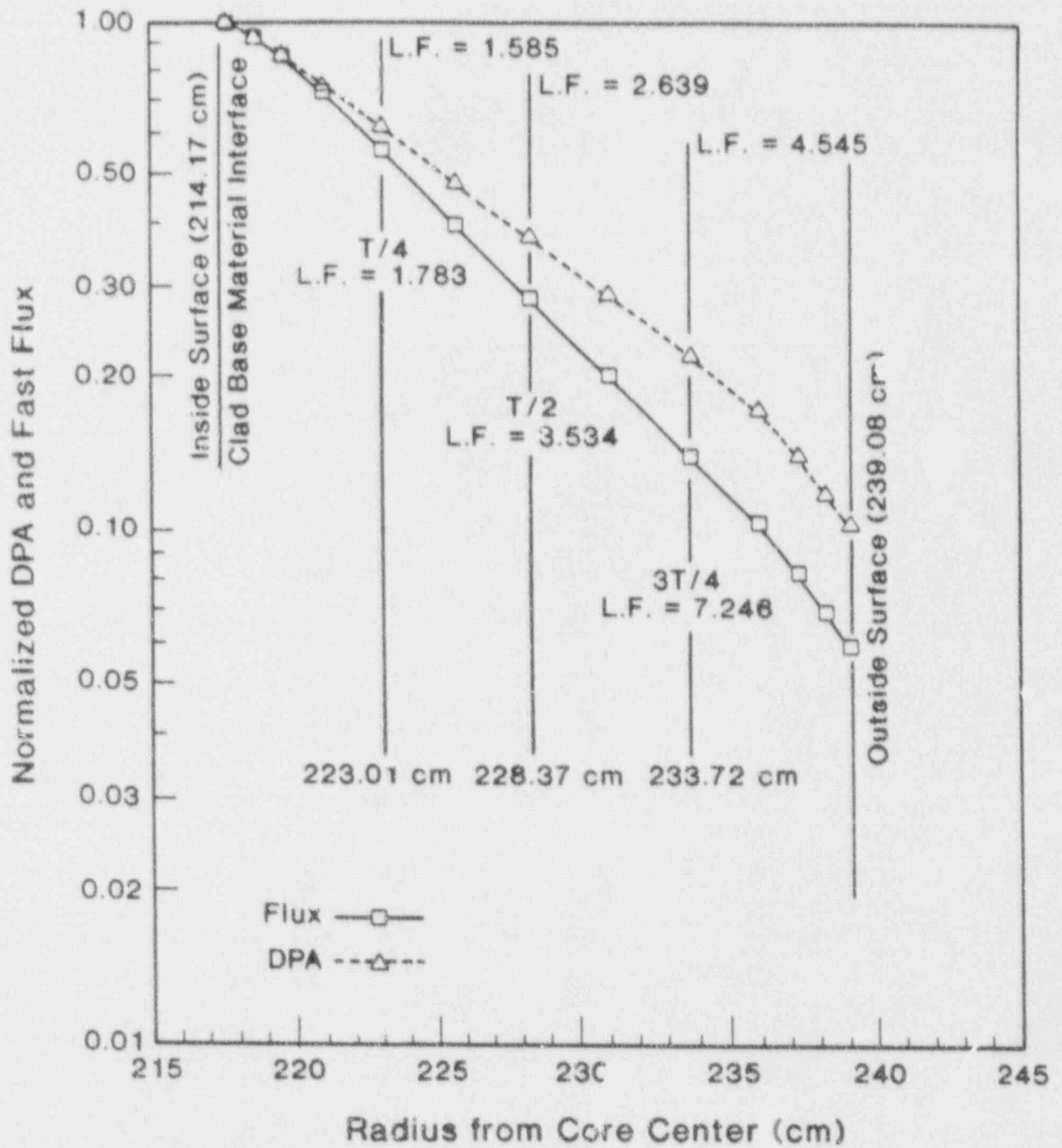
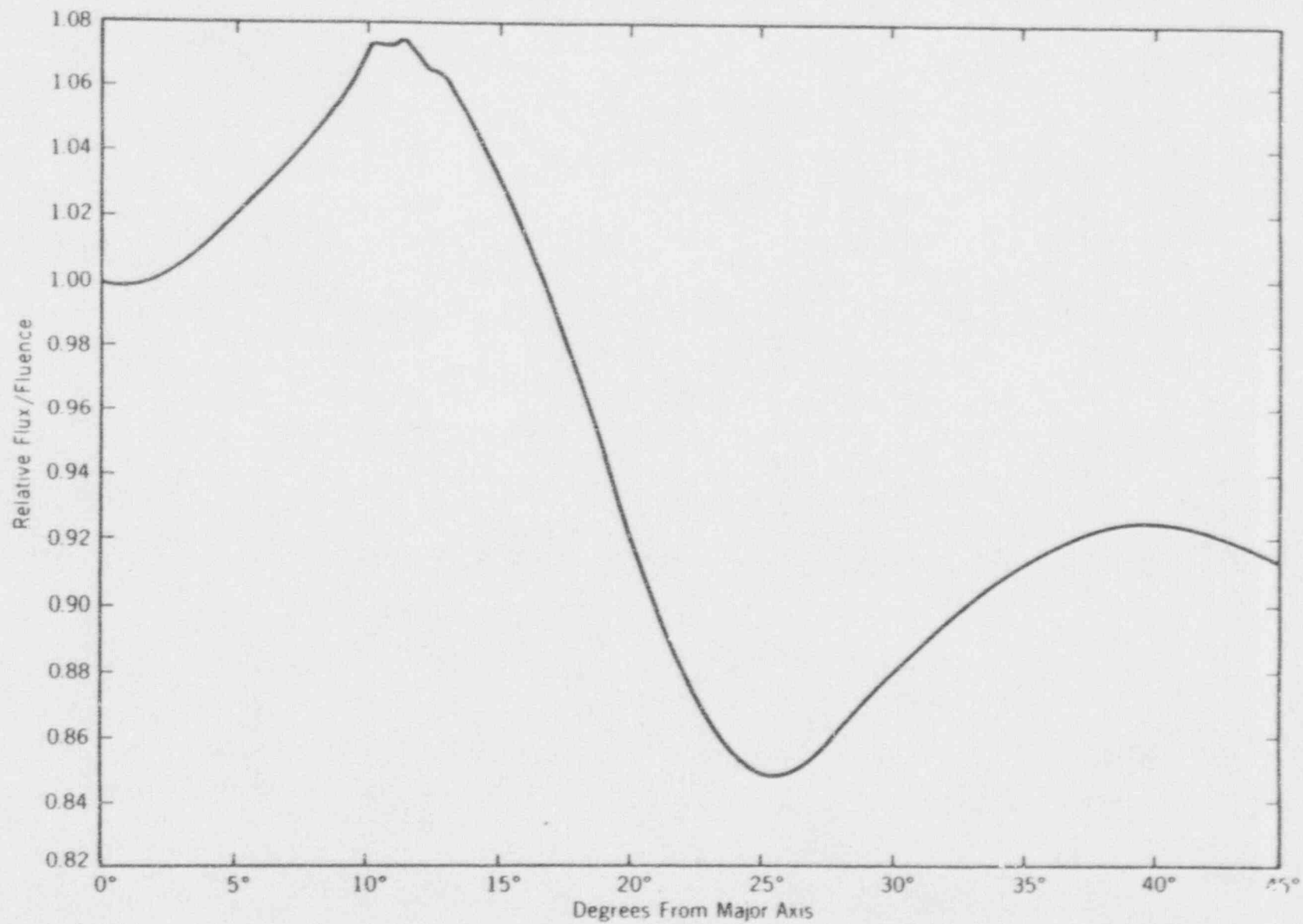


Figure 6-3. Azimuthal Flux and Fluence Distributions at Reactor Vessel Inside Surface



6-11

7. DISCUSSION OF CAPSULE RESULTS

7.1. Pre-Irradiation Property Data

A review of the unirradiated properties of the reactor vessel core beltline region materials indicated no significant deviation from expected properties except in the case of the upper-shelf properties of the weld metal. Based on the predicted end-of-service peak neutron fluence value at the 1/4T vessel wall location and the copper content of the weld metal, it was predicted that the end-of-service Charpy upper shelf energy (USE) would be below 50 ft-lb. Weld metal representative of the controlling weld metal was selected for inclusion in the surveillance program in accordance with the criteria in effect at the time the program was designed for Oconee Unit-3. The applicable selection criterion was based on the unirradiated properties only.

7.2. Irradiated Property Data

7.2.1. Tensile Properties

Table 7-1 compares irradiated and unirradiated tensile properties. At both room temperature and elevated temperature, the ultimate and yield strength changes in the base metal as a result of irradiation and the corresponding changes in ductility are within the limits observed for similar materials. There is some strengthening, as indicated by increases in ultimate and yield strengths and decreases in ductility properties. All changes observed in the base metal are such as to be considered within acceptable limits. The changes at both room temperature and 580F in the properties of the weld metal are larger than those observed for the base metal, indicating a greater sensitivity of the weld metal to irradiation damage. In either case, the changes in tensile properties are insignificant relative to the analysis of the reactor vessel materials at this period in service life.

A comparison of the tensile data from previously evaluated capsules (Capsules OCIII-A and OCIII-B) with the corresponding data from the capsule reported in this report is shown in Table 7-2. The currently reported capsule experienced a fluence that is twelve times greater than the first capsule.

The general behavior of the tensile properties as a function of neutron irradiation is an increase in both ultimate and yield strength and a decrease in ductility as measured by both total elongation and reduction of area. The most significant observation from these data is that the weld metal exhibited greater sensitivity to neutron radiation than the base metal.

7.2.2. Impact Properties

The behavior of the Charpy V-notch impact data is more significant to the calculation of the reactor system's operating limitations. Table 7-3 compares the observed changes in irradiated Charpy impact properties with the predicted changes.

The 30 ft-lb transition temperature shift for the base metal is not in good agreement with the value predicted using either Regulatory Guide 1.99, Rev. 2¹⁷ even without applying the margin which is required. It would be expected that these values would exhibit better agreement when it is considered that the data used to develop Regulatory Guide 1.99, Rev. 2, was taken at the 30 ft-lb temperature.

The transition temperature measurements at 30 ft-lbs for the weld metal is not in good agreement with the results using Regulatory Guide 1.99, Revision 2 without the margin applied. With the addition of the margin the procedure is very conservative in predicting the irradiated values. The estimating curves of Regulatory Guide 1.99, Rev. 2, are conservative for predicting the 30 ft-lb transition temperature shifts since the procedure requires that a margin be added to the calculated value to provide a conservative value.

The data for the decrease in Charpy USE with irradiation showed good agreement with predicted values for the base metal and only fair agreement for the weld metal. However, a good comparison of the measured data with the predicted value is not expected in view of the lack of data for low-, medium-, or high-

copper-content materials at the fluence values that were used to develop the estimating curves.

A comparison of the Charpy impact data from the previously evaluated capsules (Capsules OCIII-A and OCIII-B) with the corresponding data from the capsule reported in this report is shown in Table 7-4. The currently reported data experienced a fluence that is eighteen times greater than the first capsule.

The base metal exhibited shifts at the 30 ft-lb level for the latest capsule that were similar to those of the previous capsules. The corresponding data for the weld metal showed a further increase at the 30 ft-lb level. This may be due to a further decrease in the upper shelf energy with a corresponding increased shift at the 30 ft-lb level.

Both the base metal and the weld metal exhibited a decrease in the upper shelf values similar to the previous capsule. The weld metal in this capsule exhibited a slightly greater decrease than the weld metal in the previous capsule. These data confirm that the upper-shelf drop for this weld metal did not reach saturation as observed in the results of capsules evaluated by others. This behavior of Charpy USE drop for this weld metal should not be considered indicative of a similar behavior of upper shelf region fracture toughness properties. This behavior indicates that other reactions may be taking place within the material besides simple neutron damage. Verification of this relationship must await the testing and evaluation of the data from compact fracture toughness test specimens.

Results from other surveillance capsules also indicate that RT_{NDT} estimating curves have greater inaccuracies than originally thought. These inaccuracies are a function of a number of parameters related to the basic data available at the time the estimating curves are established. These parameters may include inaccurate fluence values, poor chemical composition values, and variations in data interpretation. The change in the regulations requiring the shift measurement to be based on the 30 ft-lb value has minimized the errors that result from using the 50 ft-lb data base to predict the shift behavior at 30 ft-lbs.

An evaluation of the reactor vessel end-of-life upper-shelf energy for each of the materials used in the fabrication was made and the results are presented in Table 7-6. This evaluation was made because the weld metals used to fabricate the reactor vessel are Linde 80 flux, low-upper-shelf-energy, relative high copper and are expected to be highly sensitive to neutron radiation damage. Two methods were used to evaluate the radiation induced decrease in upper shelf energy. The method of Regulatory Guide 1.99, Revision 2, which is the same procedure as used in Revision 1, and the method presented in BAW-1803¹⁸ which was developed specifically to address the need of an estimating method for this class of weld metals.

The methods of Regulatory Guide 1.99, Revision 2, indicate that two of the welds may be expected to decrease below 50 ft-lb level prior to EOL. However, BAW-1803 shows that none of the materials used in the fabrication of the reactor vessel will have an upper-shelf energy below 50 ft-lbs through 32 EFPY design life based on the T/4 wall location. Regulatory Guide 1.99 method also predicts a decrease below 50 ft-lbs for the controlling weld metal at the vessel inside wall.

copper-content materials at the fluence values that were used to develop the estimating curves.

A comparison of the Charpy impact data from the previously evaluated capsules (Capsules OCIII-A and OCIII-B) with the corresponding data from the capsule reported in this report is shown in Table 7-4. The currently reported data experienced a fluence that is eighteen times greater than the first capsule.

The base metal exhibited shifts at the 30 ft-lb level for the latest capsule that were similar to those of the previous capsules. The corresponding data for the weld metal showed a further increase at the 30 ft-lb level. This may be due to a further decrease in the upper shelf energy with a corresponding increased shift at the 30 ft-lb level.

Both the base metal and the weld metal exhibited a decrease in the upper shelf values similar to the previous capsule. The weld metal in this capsule exhibited a slightly greater decrease than the weld metal in the previous capsule. These data confirm that the upper-shelf drop for this weld metal did not reach saturation as observed in the results of capsules evaluated by others. This behavior of Charpy USE drop for this weld metal should not be considered indicative of a similar behavior of upper shelf region fracture toughness properties. This behavior indicates that other reactions may be taking place within the material besides simple neutron damage. Verification of this relationship must await the testing and evaluation of the data from compact fracture toughness test specimens.

Results from other surveillance capsules also indicate that RT_{NDT} estimating curves have greater inaccuracies than originally thought. These inaccuracies are a function of a number of parameters related to the basic data available at the time the estimating curves are established. These parameters may include inaccurate fluence values, poor chemical composition values, and variations in data interpretation. The change in the regulations requiring the shift measurement to be based on the 30 ft-lb value has minimized the errors that result from using the 50 ft-lb data base to predict the shift behavior at 30 ft-lbs.

The design curves for predicting the shift will continue to be modified as more data become available; until that time, the design curves for predicting the RT_{NDT} shift as given in Regulatory Guide 1.99, Revision 2, are considered adequate for predicting the RT_{NDT} shift of those materials for which data are not available. These curves will be used to establish the pressure-temperature operational limitations for the irradiated portions of the reactor vessel until the time that new prediction curves are developed and approved.

The lack of good agreement of the change in Charpy USE is further support of the inaccuracy of the prediction curves. Although the prediction curves are conservative in that they generally predict a larger drop in upper-shelf than is observed for a given fluence and copper content, the conservatism can unduly restrict the operational limitations. These data support the contention that the USE drop curves will have to be revised as more reliable data become available; until that time the design curves used to predict the decrease in USE of the controlling materials are considered conservative.

7.3. Reactor Vessel Fracture Toughness

An evaluation of the reactor vessel end-of-life fracture toughness and the pressurized thermal shock criterion was made and the results are presented in Table 7-5.

The fracture toughness evaluation shows that the controlling weld metal may have an end-of-life RT_{NDT} of 228F based on Regulatory Guide 1.99, Revision 2. This predicted shift is excessive since the latest capsule (Capsule OCIII-D) exhibited a measured shift of 140F for a fluence of 1.45×10^{19} n/cm². Ratioing this measured shift to the T/4 wall location fluence, it is estimated that the end-of-life RT_{NDT} shift will be significantly less than the value predicted using Regulatory Guide 1.99, Revision 2. This reduced shift permits the calculation of less restrictive pressure temperature operating limitations than if Regulatory Guide 1.99, Revision 2, was used.

The pressurized thermal shock evaluation demonstrates that the Oconee Unit 3 reactor pressure vessel is well below the screening criterion limits and, therefore, need not take any additional corrective action as required by the regulation.

An evaluation of the reactor vessel end-of-life upper-shelf energy for each of the materials used in the fabrication was made and the results are presented in Table 7-6. This evaluation was made because the weld metals used to fabricate the reactor vessel are Linde 80 flux, low-upper-shelf-energy, relative high copper and are expected to be highly sensitive to neutron radiation damage. Two methods were used to evaluate the radiation induced decrease in upper shelf energy. The method of Regulatory Guide 1.99, Revision 2, which is the same procedure as used in Revision 1, and the method presented in BAW-1803¹⁸ which was developed specifically to address the need of an estimating method for this class of weld metals.

The methods of Regulatory Guide 1.99, Revision 2, indicate that two of the welds may be expected to decrease below 50 ft-lb level prior to EOL. However, BAW-1803 shows that none of the materials used in the fabrication of the reactor vessel will have an upper-shelf energy below 50 ft-lbs through 32 EFPY design life based on the T/4 wall location. Regulatory Guide 1.99 method also predicts a decrease below 50 ft-lbs for the controlling weld metal at the vessel inside wall.

Table 7-1. Comparison of Capsule OCIII-D Tension Test Results

	<u>Room Temp. Test</u>		<u>Elevated Temp. Test (580F)</u>	
	<u>Unirr</u>	<u>Irrad</u>	<u>Unirr</u>	<u>Irrad</u>
<u>Base Metal -- ANK-191, Transverse</u>				
Fluence, 10^{19} n/cm ² (> 1 MeV)	0	1.45	0	1.45
Ultimate tensile strength, ksi	85.4	91.5	85.0	87.2
0.2% yield strength, ksi	63.1	66.9	55.7	60.3
Uniform elongation, %	13.8	9.9	11.9	9.9
Total elongation, %	30.4	26.6	28.6	23.3
Reduction of area, %	66.8	65.1	66.5	62.0
<u>Weld Metal -- WF-209-1</u>				
Fluence, 10^{19} n/cm ² (> 1 MeV)	0	1.45	0	1.45
Ultimate tensile strength, ksi	90.5	111.3	87.9	102.9
0.2% yield strength, ksi	75.0	98.0	67.4	86.6
Uniform elongation, %	12.5	10.7	10.9	9.0
Total elongation, %	28.1	24.2	21.4	17.7
Reduction of area, %	62.9	56.7	52.1	49.4

Table 7-2. Summary of Oconee Unit 3 Reactor Vessel Surveillance Capsules Tensile Test Results

Material	Fluence 10^{18} n/cm ²	Test Temp, F	Strength, ksi				Ductility, %			
			Ultimate	% ^(*)	Yield	% ^(*)	Total Elong.	% ^(*)	Reduction of Area	% ^(*)
Base Metal (ANK-191)	0	70	85.4	-	63.1	-	30	-	67	-
		580	85.0	-	55.7	-	29	-	67	-
	0.81	70	87.5	+ 2.5	63.0	- 0.2	30	00	68	+ 1.5
		580	86.4	+ 1.6	57.2	+ 2.7	29	00	67	0.0
	3.12	69	105.6	+23.7	91.3	+44.7	25	-16.7	56	-16.4
		585	86.9	+ 2.2	56.0	+ 0.1	37	+27.6	64	- 4.5
	14.50	70	91.5	+ 7.1	66.9	+ 6.0	27	-10.0	65	- 3.0
		550	87.2	+ 2.6	60.3	+ 8.3	23	-20.7	62	- 7.5
7-7 Weld Metal (WF-209-1)	0	70	90.5	-	75.0	-	28	-	63	-
		580	87.9	-	67.4	-	21	-	52	-
	0.81	70	93.9	+ 3.8	79.3	+ 5.7	27	- 3.6	63	0.0
		580	93.7	+ 6.6	72.6	+ 7.7	23	+ 9.5	60	+15.4
	3.12	69	105.0	+16.6	90.6	+20.8	25	-10.7	57	- 4.8
		585	85.6	- 2.6	57.8	-14.2	26	+23.8	56	+ 7.7
	14.50	70	111.3	+23.0	98.0	+30.7	24	-14.3	57	- 9.5
		550	102.9	+17.1	86.6	+28.5	18	-16.7	49	- 5.8

(*) Change relative to unirradiated.

Table 7-3. Observed Vs. Predicted Changes for Capsule OCIII-D Irradiated Charpy Impact Properties - 1.45×10^{19} n/cm² (E > 1 MeV)

Material	Observed	Predicted RG 1.99/2 ^(a)	Predicted RG 1.99/2+M ^(b)
<u>Increase in 30 ft-'b Trans. Temp., F</u>			
Base material (ANK-19')			
Transverse	31	22	33
Heat-affected zone	74	22	33
Base material (AWS-192)			
Transverse	45	22	33
Heat-affected zone	1	22	33
Weld metal (WF-209-1)	140	196	252
Correlation material (HSST plate 02)	119	141	197
<u>Decrease in Charpy USE, ft-lb</u>			
Base material (ANK-191)			
Transverse	19	17	N.A.
Heat-affected zone	22	11	N.A.
Base material (AWS-192)			
Transverse	19	12	N.A.
Heat-affected zone	6	13	N.A.
Weld metal (WF-209-1)	24	30	N.A.
Correlation material (HSST plate 02)	36	36	N.A.

(a) Per R.G. 1.99, Revision 2, May 1988.

(b) Per R.G. 1.99, Revision 2, May 1988, plus 2 x margin.

Table 7-4. Summary of Oconee Unit 3 Reactor Vessel Surveillance Capsules Charpy Impact Test Results

Material	Fluence, 10^{18} n/cm ²	Transition Temperature Increase, F			Upper-Shelf Energy, ft-lb	
		30 ft-lb Observed	Predicted 30 ft-lb ^(a)	Predicted 30 ft-lb ^(b)	Observed	Predicted ^(a)
Base material (ANK-191)						
Transverse	0.81	9	8	12	130	136
	3.12	32	14	21	123	131
	14.50	31	22	33	125	127
Heat-affected zone	0.81	0	8	12	145	85
	3.12	Ind.	14	21	67	82
	14.50	74	22	33	68	79
Base material (AWS-192)						
Transverse	0.81	63	8	12	100	108
	3.12	19	14	21	99	103
	14.50	45	22	33	93	100
Heat-affected zone	3.12	Ind.	14	21	123	105
	14.50	1	22	33	108	101
Weld metal (WF-209-1)	0.81	48	70	105	54 ^(d)	50
	3.12	64	121	177	49 ^(d)	44
	14.50	140	196	252	42 ^(d)	36
Correlation material (HSST plate 02)	3.12	39	87	131	96	104
	14.50	119	141	197	94	94

(a) Per R.G. 1.99, Revision 2, May 1988.

(b) Per R.G. 1.99, Revision 2, plus margin.

(c) Per BAW-1803, Revision 1, dated March 1991, plus margin.¹⁸

(d) Upper-shelf energy value re-defined per ASTM E185.

Table 7-5. Evaluation of Reactor Vessel End-of-Life Fracture Toughness and Pressurized Thermal Shock Criterion - Duke Power Company, Oconee Unit-3 (32 EFY)

Material Description Reactor Vessel Bellline Region Location	Heat Number	Type	Material Chemical Composition		Estimated EOL Fluence		T/4 Wall EOL RT _{nor} , F		PTS Evaluation, f ⁶⁰		
			Copper, w/o	Nickel, w/o	Inside Surface n/cm ²	T/4 Wall Location n/cm ²	Per RG 1.99/2 ⁶⁰	Per BAW 1803/1 ⁶⁰	Initial RT _{nor}	EOL RT _{nor}	Screening Criterion
Lower nozzle bell	RDM4680	SAS08, C12	0.13	0.91	7.21E+18	4.05E+18	144	N.A.	(+3)	138	270
Upper shell	AMS-192	SAS08, C12	0.01	0.73	9.49E+18	5.33E+18	53	N.A.	+20	74	270
Lower shell	ANK-191	SAS08, C12	0.02	0.76	9.49E+18	5.33E+18	53	N.A.	+20	74	270
Upper circum. weld	WF-200	Weld	0.24	0.63	7.21E+18	4.05E+18	202	117	0	228	300
Mid. circum. weld (I.D. 75%)	WF-67	Weld	0.24	0.50	9.49E+18	5.33E+18	208	189	-3	223	300
Mid. circum. weld (O.D. 25%)	WF-70	Weld	0.35	0.59	N.A.	N.A.	N.A.	N.A.	N.A.	N.A.	N.A.
Lower circum. weld	WF-169-1	Weld	0.18	0.63	5.31E+16	2.98E+16	Neg.	Neg.	0	77	300

⁶⁰Per Regulatory Guide 1.99, Revision 2, dated May 1988.

⁶¹Per BAW 1803, Revision 1, dated March 1991.

⁶²Per 10CFR50, Section 50.61, Fracture Toughness Requirements for Protection Against Pressurized Thermal Shock Events with proposed changes to make it consistent with Regulatory Guide 1.99, Revision 2, May 1988 (proposed revision published in Federal Register, Vol. 54, No. 245, December 26, 1989).

Table 7-6. Evaluation of Duke Power Company Oconee Unit-3 Reactor Vessel End-of-Life (32 EFPY) Upper-Sheaf Energy

Material Description Reactor Vessel Beltline Region Location	Heat Number	Type	Material Chemical Composition		Estimated E/NL Fluence		Initial USE ft-lbs	Estimated EOL-USE per RG 1.99/2 ^m		Estimated EOL-USE per BAW-1803/1 ^m		Estimated EFPY to 50 ft-lbs at 1/4 Location RG 1.99/2 BAW-1803/1	
			Copper w/o	Nickel w/o	Inside Surface n/cm ²	1/4 Wall Location n/cm ²		Inside Surface	1/4 Wall Location	Inside Surface	1/4 Wall Location		
Lower nozzle belt	ROM4680	SA503, C12	0.13	0.91	7.21E+18	4.05E+18	(133) ^m	106	109	N.A.	N.A.	>32	N.A.
Upper shell	AMS-192	SA508, C12	0.01	0.73	9.49E+18	5.33E+18	97 ^m	87	89	N.A.	N.A.	>32	N.A.
Lower shell	ARK-191	SA508, C12	0.02	0.76	9.49E+18	5.33E+18	123 ^m	110	111	N.A.	N.A.	>32	N.A.
Upper circum. weld	WF-200	Weld	0.24	0.63	7.21E+18	4.05E+18	(70) ^m	45	48	53	54	21	>32
Mid. circum. weld (10 75%)	WF-67	Weld	0.24	0.60	9.49E+18	5.33E+18	(70) ^m	44	47	52	54	16	>32
Mid. circum. weld (00 25%)	WF-70	Weld	0.35	0.59	N.A.	N.A.	N.A.	N.A.	N.A.	N.A.	N.A.	N.A.	N.A.
Lower circum. weld	WF-169	Weld	0.18	0.63	5.31E+16	2.98E+16	(70) ^m	N.A.	N.A.	N.A.	N.A.	>32	>32

^mPer Regulatory Guide 1.99, Revision 2, dated May 1988.
ⁿEstimated per BAW-1803, Revision 1, dated March 1991.
^oPer Certified Materials Test Reports.
^pEstimated per BAW-10046P, dated March 1976.

8. DETERMINATION OF REACTOR COOLANT PRESSURE BOUNDARY PRESSURE - TEMPERATURE LIMITS

The pressure-temperature limits of the reactor coolant pressure boundary (RCPB) of Oconee Unit-3 are established in accordance with the requirements of 10CFR50, Appendix G. The methods and criteria employed to establish operating pressure and temperature limits are described in topical report BAW-10046A.¹⁹ The objective of these limits is to prevent nonductile failure during any normal operating condition, including anticipated operation occurrences and system hydrostatic tests. The loading conditions of interest include the following:

1. Normal operations, including heatup and cooldown.
2. Inservice leak and hydrostatic tests.
3. Reactor core operation.

The major components of the RCPB have been analyzed in accordance with 10CFR50, Appendix G. The closure head region, the reactor vessel outlet nozzle, and the beltline region have been identified as the only regions of the reactor vessel (and consequently of the RCPB) that regulate the pressure-temperature limits. Since the closure head region is significantly stressed at relatively low temperatures (due to mechanical loads resulting from bolt preload), this region largely controls the pressure-temperature limits of the first several service periods. The reactor vessel outlet nozzle also affects the pressure-temperature limit curves of the first several service periods. This is due to the high local stresses at the inside corner of the nozzle, which can be two to three times the membrane stresses of the shell. After the first several years of neutron radiation exposure, the RT_{NDT} of the beltline region materials will be high enough that the beltline region of the reactor vessel will start to control the pressure-temperature limits of the RCPB. For the service period for which the limit curves are established, the maximum allowable pressure as a function of fluid temperature is obtained through a point-by-point comparison of the limits

imposed by the closure head region, the outlet nozzle, and the beltline region. The maximum allowable pressure is taken to be the lowest of the three calculated pressures.

The limit curves for Oconee Unit-3 are based on the predicted values of the adjusted reference temperatures of all the beltline region materials at the end of fifteenth EFPY. The fifteenth EFPY was selected as the last time period because it represents a logical sequence from the previous analysis and the surveillance capsule was scheduled to be withdrawn at the end of the refueling cycle when the estimated capsule fluence corresponded to approximately the inside surface end-of-life value. However, the use of low-leakage fuel cycles caused the capsule fluence to exceed the reactor vessel inside surface end-of-life fluence. The time difference between the withdrawal of this surveillance capsule and future operating requirements provides adequate time for re-establishing the operating pressure and temperature limits for subsequent periods of operation beyond the current surveillance capsule withdrawal.

The unirradiated impact properties were determined for the surveillance beltline region materials in accordance with 10CFR50, Appendixes G and H. For the other beltline region and RCPB materials for which the measured properties are not available, the unirradiated impact properties and residual elements, as originally established for the beltline region materials, are listed in Table A-1. The adjusted reference temperatures are calculated by adding the predicted radiation-induced RT_{NDT} and the unirradiated RT_{NDT} . The predicted RT_{NDT} is calculated using the respective neutron fluence and copper and nickel contents. Figure 8-1 illustrates the calculated peak neutron fluence at several locations through the reactor vessel beltline region wall. The supporting information for Figure 8-1 is described in Section 6. The neutron fluence values of Figure 8-1 are the predicted fluences that have been demonstrated (Section 6) to be conservative. The design curves of Regulatory Guide 1.99, Rev. 2, were used to predict the radiation-induced RT_{NDT} values as a function of the material's copper and nickel content and neutron fluence.

The neutron fluences and adjusted RT_{NDT} values of the beltline region materials at the end of the fifteenth full-power year are listed in Table 8-1. The neutron fluences and adjusted RT_{NDT} values are given for the 1/4T and 3/4T vessel wall

locations (T = wall thickness). The assumed RT_{NDT} of the closure head region and the outlet nozzle steel forgings is 60F, in accordance with BAW-10046. The RT_{NDT} values selected for calculation of the pressure-temperature limit curves are those values which exhibit the highest values at the T/4 and 3T/4 locations. In the case of the 3T/4 location, one weld metal made up the outside 25% of the weldment and another made up the remainder. It was assumed that the theoretical T/4 thickness flaw used to calculate the pressure-temperature curves layed such that its forward most crack front was posed to enter the material composing the major portion at the weldment and, therefore, that material is controlling.

Figure 8-2 shows the reactor vessel's pressure-temperature limit curves for normal heatup. This figure also shows the the core criticality limits as required by 10CFR50, Appendix G. Figure 8-3 shows the vessel's pressure-temperature limit curves for normal cooldown. Figure 8-4 shows the vessel's heatup and cooldown limitations during inservice leak and hydrostatic tests. All pressure-temperature limit curves are applicable up to the fifteenth EFPY as indicated. Protection against nonductile failure is ensured by maintaining the coolant pressure below the upper limits of the pressure-temperature limit curves. The acceptable pressure and temperature combinations for reactor vessel operation are below and to the right of the limit curve. The reactor is not permitted to go critical until the pressure-temperature combinations are to the right of the criticality limit curve. To establish the pressure-temperature limits for protection against nonductile failure of the RCPB, the limits presented in Figures 8-2 through 8-4 must be adjusted by the pressure differential between the point of system pressure measurement and the pressure on the reactor vessel controlling the limit curves. This is necessary because the reactor vessel is the most limiting component of the RCPB.

Table 8-1. Data for Preparation of Pressure-Temperature Limit Curves for Oconee Nuclear Station - Unit-3 -- Applicable Through 15 EFPI

Material Identification Heat No.	Material Type	Beltline Region Location	Weldment Location		Inside Surface Fluency n/cm ² (g)	Chemical Composition (d)		Chemistry Factor	Initial RT _{NDT} F	Radiation Induced RT _{NDT} at 15 EFPI F 1/4 31/4	Margin, F	Adjusted RT _{NDT} (a) at End of 15 EFPI F 1/4 31/4
			Core Midplane to Weld cm	Location from Major Axis Degrees		Copper, w/o	Nickel, w/o					
ROR 4680	SASOB, C12	Lower nozzle belt	---	---	3.84E+18	0.13	0.91	96	(+3)(c)	58 37	69/69	130 109
AMS-192	SASOB, C12	Upper shell	---	---	5.05E+18	0.01	0.73	20	+20(g)	13 9	14/10	47 39
AMS-191	SASOB, C12	Lower shell	---	---	5.05E+18	0.02	0.76	20	+20(g)	13 9	14/10	47 39
WF-200	ASA/Linde 80	Upper circ. weld (100%)	123	---	3.84E+18	0.24	0.63	178	(-5)(b)	108 68	69/69	172 132
WF-67	ASA/Linde 80	Mid. circ. weld (10 75%)	63	---	5.05E+18	0.24	0.60	173	(-5)(b)	116 75	69/69	[190](f) [139](f)
WF-70	ASA/Linde 80	Mid. circ. weld (100 25%)	63	---	5.05E+18	0.35	0.59	211	(-5)(b)	...	0/69	...
WF-169-1	ASA/Linde 80	Lower circ. weld (100%)	-249	---	3.03E+16	0.18	0.63	159	(-5)(b)	N.A. N.A.

(a) RT_{NDT} calculated per Regulatory Guide 1.99, Revision 2, dated May 1982.

(b) Estimated initial RT_{NDT} of weld metals per BAW-1803, Revision 1, March 1991; One Standard Deviation = 20F.

(c) Estimated initial RT_{NDT} of base metals per BAW-10046P, March 1976.

(d) Materials chemical compositions per BAW-1820, 20 December 1984 and BAW-1799, July 1983, 21

(e) Initial calculated RT_{NDT} values for use in calculation of pressure-temperature limits (see text).

(f) RT_{NDT} values used to calculate pressure-temperature limits.

(g) Per Certified Material test Reports.

(h) See Section 6, Table 6-3.

Figure 8-1. Predicted Fast Neutron Fluence at Various Locations Through Reactor Vessel Wall for 32 EFPY - Oconee Nuclear Station, Unit-3

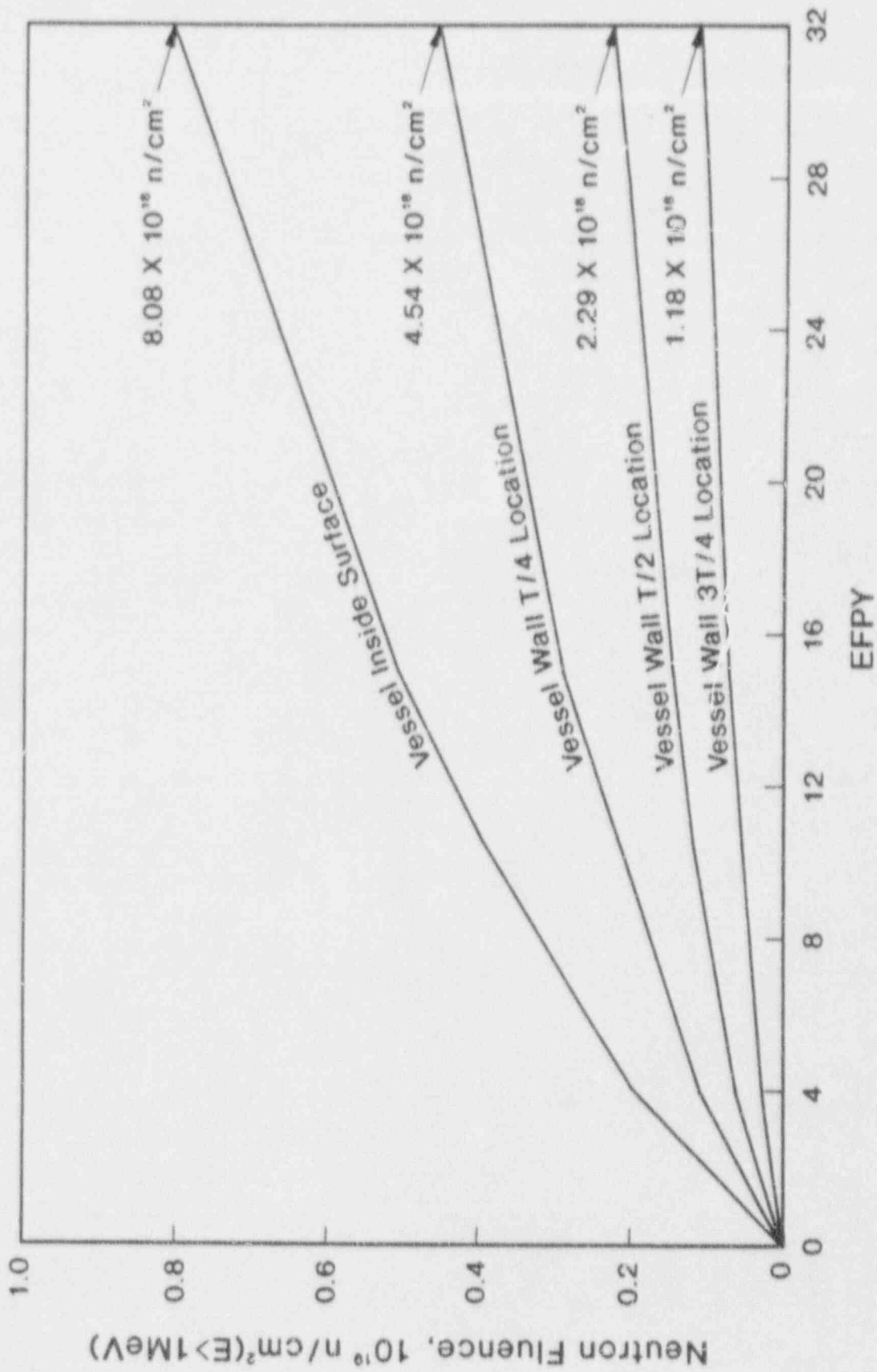


Figure 8-2. Reactor Vessel Pressure-Temperature Limit Curves for Normal Operation - Heatup, Applicable for First 15 EFPI - Oconee Nuclear Station, Unit-3

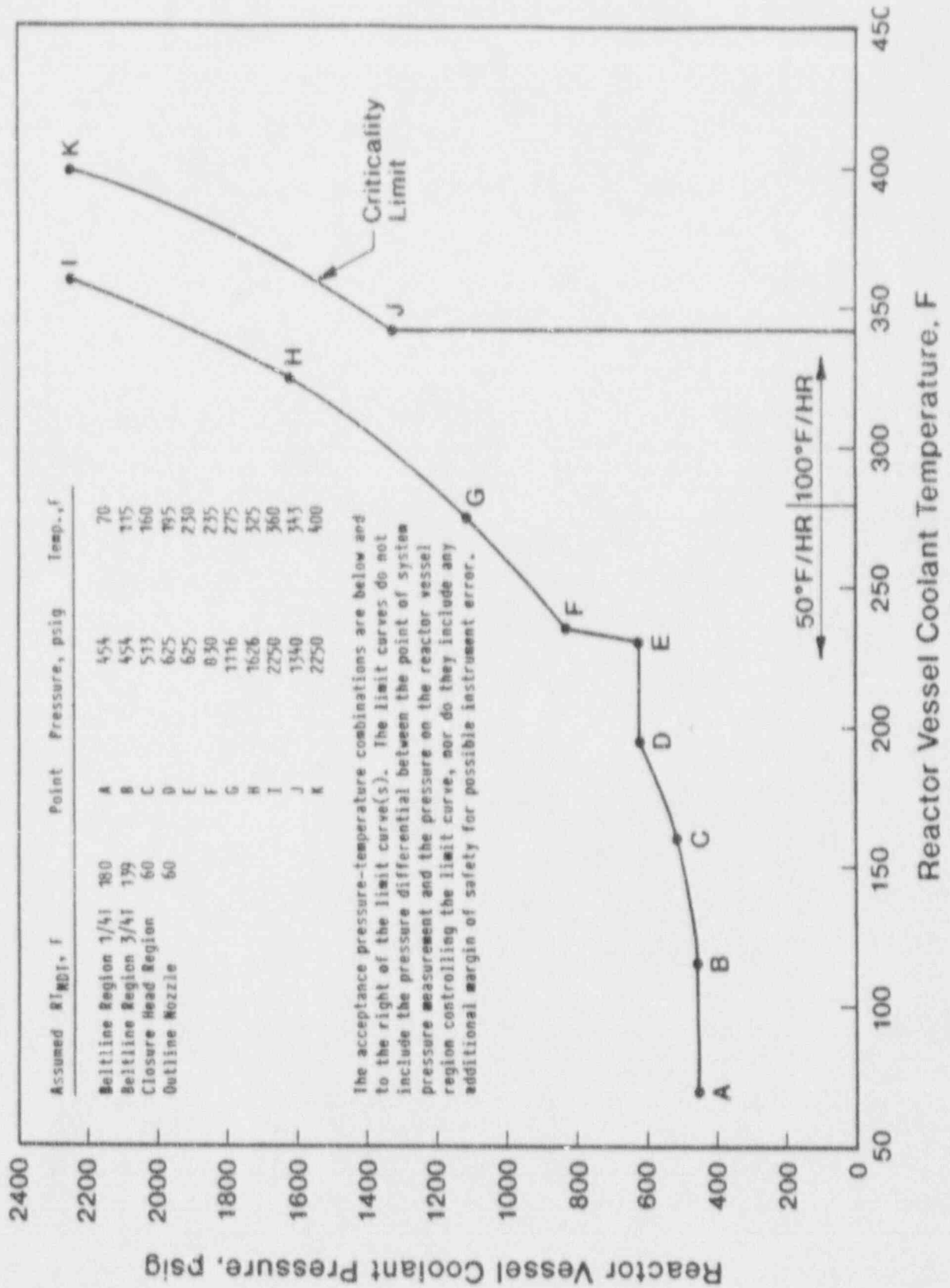
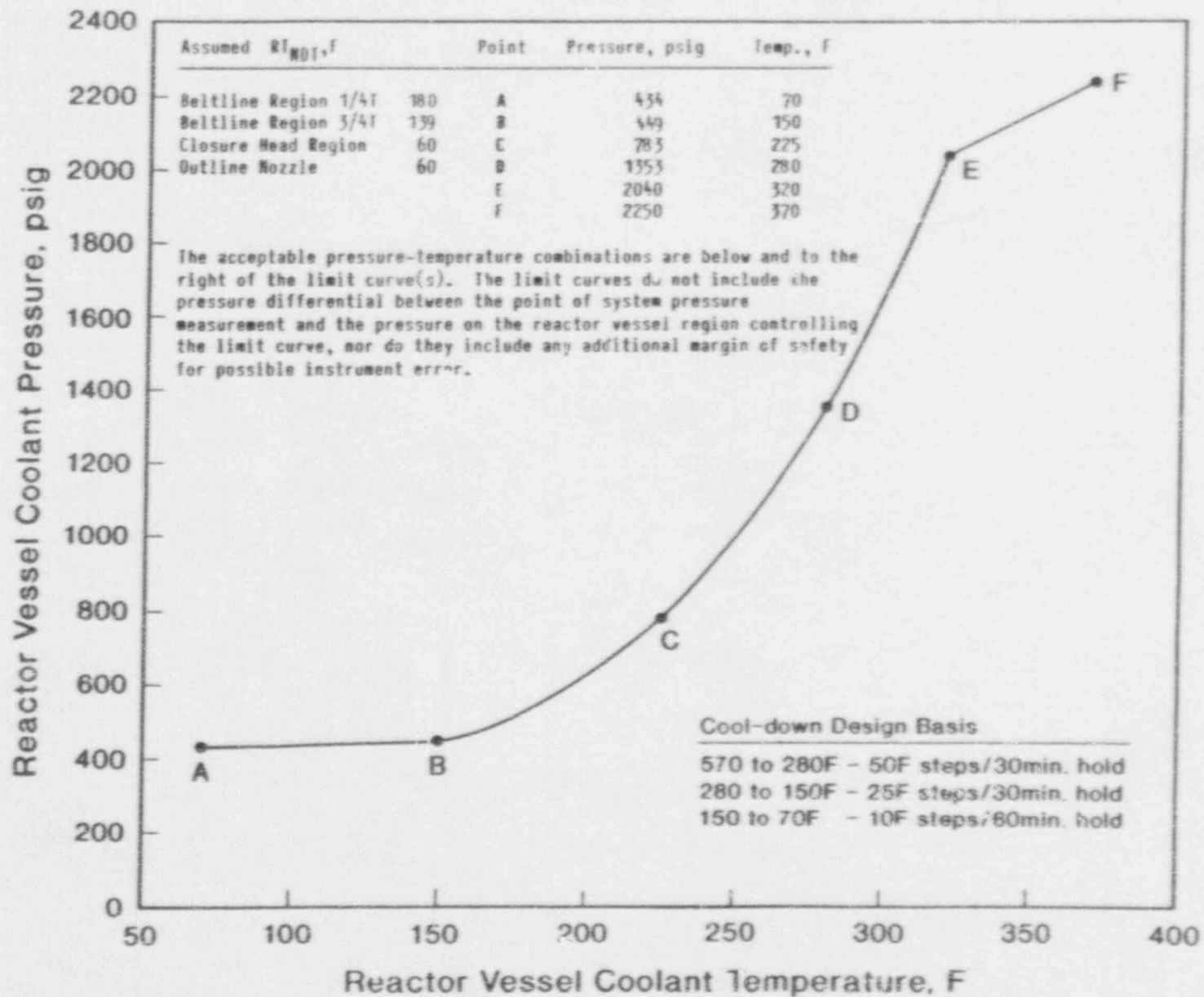
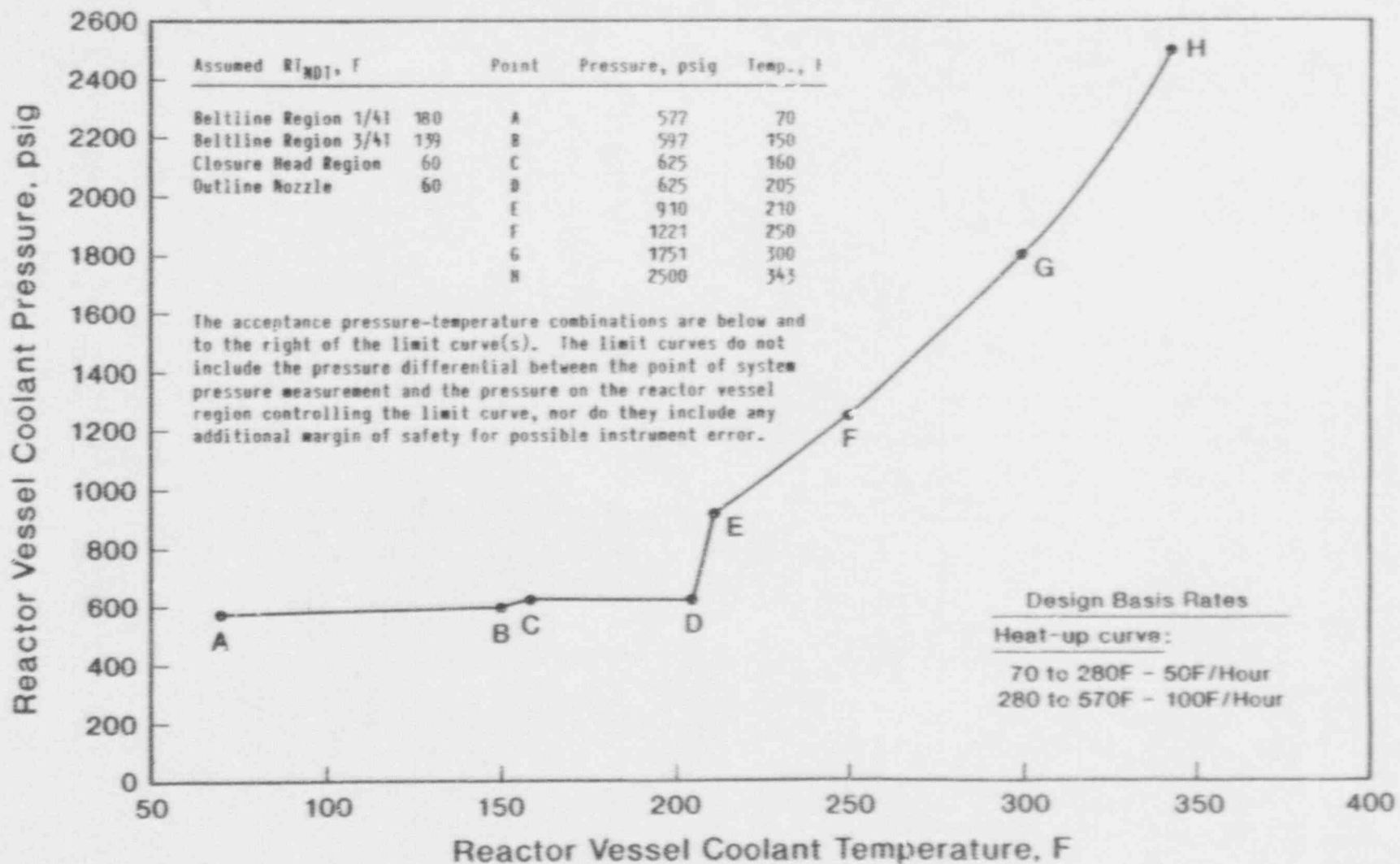


Figure 8-3. Reactor Vessel Pressure-Temperature Limit Curves for Normal Operation - Cooldown, Applicable for First 15 EFPY - Oconee Nuclear Station, Unit-3



C-7

Figure 8-4. Reactor Vessel Pressure-Temperature Limit Curves for Inservice Leak and Hydrostatic Tests, Applicable for First 15 EFPY - Oconee Nuclear Station, Unit-3



9. SUMMARY OF RESULTS

The analysis of the reactor vessel material contained in the third surveillance capsule, OCIII-D, removed for evaluation as part of the Duke Power Company, Oconee Nuclear Station Unit-3, Reactor Vessel Surveillance Program, led to the following conclusions:

1. The capsule received an average fast fluence of 1.45×10^{19} n/cm² (E > 1.0 MeV). The predicted fast fluence for the reactor vessel T/4 location at the end of the eleventh fuel cycle is 2.18×10^{18} n/cm² (E > 1 MeV).
2. The fast fluence of 1.45×10^{19} n/cm² (E > 1 MeV) increased the RT_{NDT} of the capsule reactor vessel core region shell materials a maximum of 140F.
3. Based on the calculated fast flux at the vessel wall, an 80% capacity factor and the planned fuel management, the projected fast fluence that the Oconee Unit-3 reactor pressure vessel inside surface will receive in 32 EFPY operation is 9.49×10^{18} n/cm² (E > 1 MeV).
4. The increase in the RT_{NDT} for the shell forging material was not in good agreement with that predicted by the currently used design curves of RT_{NDT} versus fluence (i.e., R.G. 1.99/Rev. 2).
5. The increase in the RT_{NDT} for the weld metal was significantly less than that predicted by the currently used design curves of RT_{NDT} versus fluence (i.e., R.G. 1.99/Rev. 2), however, the prediction techniques are conservative.
6. The RT_{PTS} values decreased for 32 EFPY because of a decrease in the estimated EOL fluence values and are below the PTS screening criteria.
7. The current techniques (i.e., Regulatory Guide 1.99, Revision 2) used to predict the change in weld metal Charpy upper-shelf properties due to irradiation are conservative.
8. The analysis of the neutron dosimeters demonstrated that the analytical techniques used to predict the neutron flux and fluence were accurate.

9. The capsule design operating temperature may have been exceeded during operating transients but not for times and temperatures that would make the capsule data unusable. The response of the surveillance capsule was representative of the conditions to which the reactor vessel experienced.

10. SURVEILLANCE CAPSULE REMOVAL SCHEDULE

Based on the postirradiation test results of capsule OCIII-D, the following schedule is recommended for examination of the remaining capsules in the Oconee Unit-3 RVSP:

Evaluation Schedule^(a)

<u>Capsule ID</u>	<u>Estimated Capsule Fluence, 10^{19} n/cm²</u>	<u>Estimated Vessel EOL Fluence, n/cm² Surface</u>	<u>1/4T</u>	<u>Estimated Date Data Available^(b)</u>
OCIII-C ^(c)	0.86	8.1E18	4.5E18	Standby
OCIII-E ^(c)	1.60	8.1E18	4.5E18	Standby
OCIII-F ^(c)	1.60	8.1E18	4.5E18	Standby

(a) In accordance with BAW-10006A and ASTM E185-82 as modified by BAW-1543A, Rev. 3.

(b) Estimated date based on 0.8 plant capacity factor.

(c) Capsules designated as standbys and will not be evaluated when removed.

11. CERTIFICATION

The specimens were tested, and the data obtained from Duke Power Company Oconee Nuclear Station Unit-3 reactor vessel surveillance Capsule OCIII-D were evaluated using accepted techniques and established standard methods and procedures in accordance with the requirements of 10CFR50, Appendixes G and H.

A. L. Lowe, Jr. 5/15/91
A. L. Lowe, Jr., P.E. Date
Project Technical Manager

This report has been reviewed for technical content and accuracy.

M. J. Devan 5/16/91
M. J. Devan (Material Properties) Date
M&SA Unit

N. L. Snidow 5/16/91
N. L. Snidow (Fluence Analysis) Date
Performance Analysis Unit

K. K. Yoon 5/16/91
K. K. Yoon, P.E. (Fracture Analysis) Date
M&SA Unit

Verification of independent review.

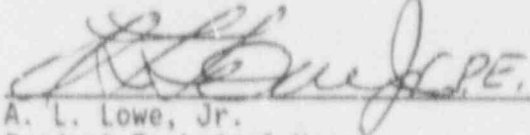
K. E. Moore 5/16/91
K. E. Moore, Manager Date
M&SA Unit

This report has been approved for release.


T. L. Baldwin 5/16/91
T. L. Baldwin Date
Program Manager


Revision 1

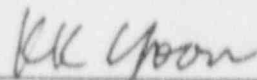
The revisions to this report were made as stated in accordance with the standard methods and procedures for the original report.


A. L. Lowe, Jr. PE. 13 May 1992
Project Technical Manager Date

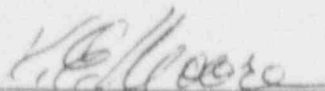
Revisions have been reviewed for technical content and accuracy.


M. J. Devan (Material Properties
M&SA Unit) 5/12/92
Date



L. Petrusa (Fluence Analysis)
Performance Analysis Unit 5/12/92
Date


K. K. Yoon P.E. (Fracture Analysis)
M&SA Unit 5/12/92
Date

Verification of independent review.


K. E. Moore, Manager
M&SA Unit 5-12-92
Date

This report approved for release.


T. L. Baldwin
Program Manager 5/12/92
Date

APPENDIX A

Reactor Vessel Surveillance Program
Background Data and Information

1. Material Selection Data

The data used to select the materials for the specimens in the surveillance program, in accordance with E-185-66, are shown in Table A-1. The locations of these materials within the reactor vessel are shown in Figure A-1.

2. Definition of Beltline Region

The beltline region of Oconee Nuclear Station Unit-3 was defined in accordance with the data given in BAW-10006A.⁴

3. Capsule Identification

The capsules used in the Oconee Unit-3 surveillance program are identified below by number and type.

Capsule Cross Reference Data

<u>ID No.</u>	<u>Type</u>
OC1111-A	V
OC1111-B	VI
OC1111-C	V
OC1111-D	VI
OC1111-E	V
OC1111-F	VI

4. Specimens Per Surveillance Capsule

See Tables A-2 and A-3.

Table A-1. Surveillance Program Material Selection Data for Oconee 3

Material Identification Heat No. Type		Beltline Region Location	Core Midplane to Weld CL, cm	Drop Weight T _{NDT} , F	Charpy Data, C _{VN}				RT T _{NDT} , F	Chemistry, %			
					Longitudinal Ø 10F, ft-lb	Transverse				Cu	P	S	Ni
						50 ft-lb	35 MLE	USE					
AMX 77	SA508 C1 2	Lower nozzle belt	--	--	90, 121, 106 103, 91, 128	--	--	--	--	0.06	0.006	0.009	0.74
AAW 163	SA508 C1 2	Upper shell	--	20	62, 77, 40	--	--	--	--	0.04	0.006	0.012	0.78
AWG 164	SA508 C1 2	Lower shell	--	20	82, 83, 90	--	--	--	--	0.02	0.010	0.010	0.78
WF-154	Weld	Circum seam	123	--	41, 37, 43	--	--	--	--	0.20	0.015	0.021	0.59
WF-25	Weld	Circum seam	- 63	--	33, 28, 49	--	--	--	--	0.29	0.019	0.010	0.71
WF-112	Weld	Circum seam	-249	--	35, 40, 30	--	--	--	--	0.22	0.024	0.006	0.58
WF-209-1A	Weld	Surv. weld	--	--	29, 30, 32	--	--	--	--	0.34	0.013	0.010	0.48

A-3

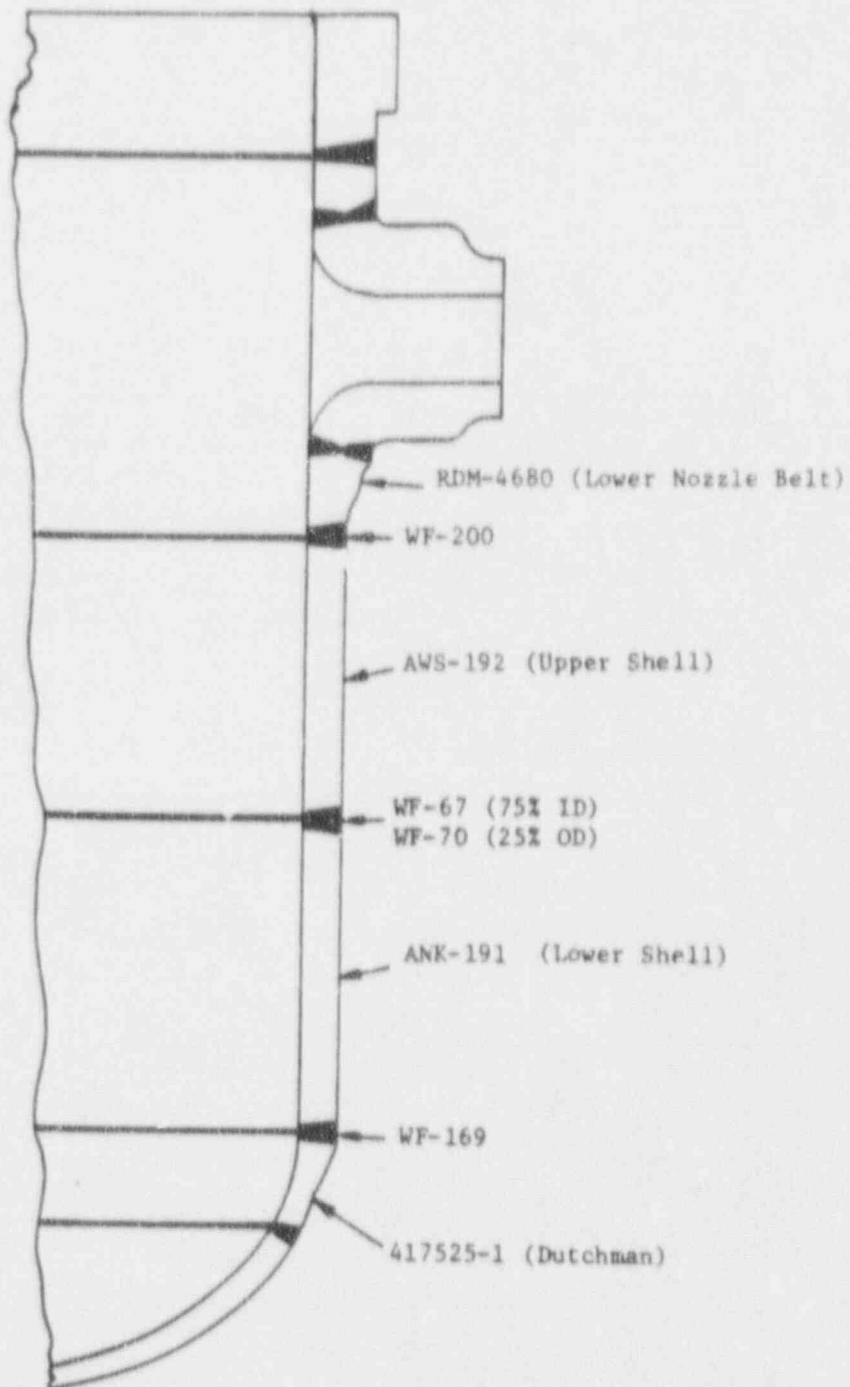
Table A-2. Materials and Specimens in Upper Surveillance Capsules OCIII-A, OCIII-C, and OCIII-E

Material Description	Number of Specimens	
	Tension	Charpy
Weld metal, WF-209-1	2	12
Heat-affected zone (HAZ)		
Heat A - ANK-191, longitudinal	0	12
Baseline material		
Heat A - ANK-191, longitudinal	0	9
Heat A - ANK-191, transverse	2	12
Heat B - AWS-192, transverse	0	9
Total per capsule	4	54

Table A-3. Materials and Specimens in Lower Surveillance Capsules OCIII-B, OCIII-D, and OCIII-F

Material Description	Number of Specimens	
	Tension	Charpy
Weld metal, WF-209-1	2	12
Weld, HAZ		
Heat A - ANK-191, longitudinal	0	12
Heat B - AWS-192, longitudinal	0	6
Baseline material		
Heat A - ANK-191, transverse	2	12
Heat B - AWS-192, transverse	0	6
Correlation HSST plate 02	0	6
Total per capsule	4	54

Figure A-1. Location and Identification of Materials Used in Fabrication of Reactor Pressure Vessel



APPENDIX B
Pre-Irradiation Tensile Data

Table B-1. Pre-Irradiation Tensile Properties of
Shell Plate Material, Heat ANK-191

Specimen No.	Test Temp, F	Strength, psi		Elongation, %		Red'n of Area, %
		Yield	Ultimate	Uniform	Total	
<u>Transverse</u>						
JJ-603	RT	70,070	85,060	13.4	30.7	66.9
604	RT	60,940	86,520	14.8	31.1	68.4
60 ^c	RT	58,310	84,730	13.3	29.3	65.1
Mean	RT	63,110	85,440	13.83	30.37	66.8
Std. dev'n.		5,040	780	0.68	0.77	0.55
JJ-607	508	56,200	85,300	12.26	28.6	66.1
510	580	56,220	85,580	13.82	28.6	61.1
611	580	54,600	84,150	9.6	28.6	67.5
Mean	580	55,670	85,010	11.89	28.6	66.57
Std. dev'n.	± 5	760	620	1.74	0	0.66

Table B-2. Pre-Irradiation Tensile Properties of
Weld Metal - Longitudinal, WF-209-1

Specimen No.	Test Temp, F	Strength, psi		Elongation, %		Red'n of Area, %
		Yield	Ultimate	Uniform	Total	
JJ-002	RT	74,630	90,460	12.5	29.3	63.2
004	RT	73,540	89,110	13.1	27.1	63.6
018	RT	76,720	91,910	11.9	27.9	62.0
Mean	RT	74,960	90,490	12.5	28.1	62.9
Std. dev'n.		1,320	1,140	0.49	0.91	0.68
JJ-001	580	67,540	87,700	10.83	20.7	52.9
011	580	66,480	88,300	11.54	22.1	53.0
013	580	68,210	87,620	10.33	21.4	50.3
Mean	580	67,410	87,870	10.9	21.4	52.07
Std. dev'n.	± 5	712	303	0.50	0.57	1.25

APPENDIX C

Pre-Irradiation Charpy Impact Data

Table C-1. Pre-Irradiation Charpy Impact Data for Shell Forging Material - Transverse Orientation, Heat ANK-191

Specimen No.	Test Temp., F	Asorbed Energy, ft-lb	Lateral Expagion, 10 ⁻³ in.	Shear Fracture, %
JJ-651	362	172	75	100
640	361	144	66	100
621	357	128	72	100
JJ-701	284	136	73	100
705	283	140	73	100
700	277	135	71	100
JJ-635	200	150	71	100
625	200	153	67	100
637	200	141	73	100
JJ-704	140	130	74	88
703	140	126	74	85
702	140	118	71	70
JJ-676	80	123	71	55
611	79	130	78	65
657	79	129	74	60
JJ-670	41	77	62	5
685	41	71	58	4
612	41	86	66	10
JJ-708	25	68	55	5
706	24	74	62	10
707	24	57	46	8
775	21	58	48	6
743	20	47	41	4
JJ-682	0.9	35	26	1
682	0.9	56	44	2
680	0.5	18	15	0
JJ-698	-39	3	2	0
697	-40	8	8	0
699	-41	14	12	0

Table C-2. Pre-Irradiation Charpy Impact Data for Shell Forging
Material - Transverse Orientation, Heat AWS-192

Specimen No.	Test Temp., F	Asorbed Energy, ft-lb	Lateral Expagion, 10^{-3} in.	Shear Fracture, %
KK-665	360	98	77	100
641	360	103	70	100
634	359	109	72	100
KK-676	282	111	71	100
677	280	106	71	100
674	279	104	70	100
KK-619	200	115	71	100
627	199	108	68	100
669	199	115	72	100
KK-683	140	119	73	100
659	140	92	71	90
679	139	113	67	100
684	139	114	71	100
KK-622	81	64	51	8
651	80	83	62	25
648	80	99	71	35
KK-675	61	80	65	40
673	60	80	64	35
678	60	64	54	25
610	60	50	44	15
KK-514	40	51	43	6
630	40	40	36	3
639	40	59	50	12
KK-657	0	37	30	<1
633	0	53	42	4
666	0	23	18	<1
KK-681	-59	2	1	0
682	-60	30	1	26
680	-60	3	2	0

Table C-3. Pre-Irradiation Charpy Impact Data for Shell Forging Material - HAZ, Transverse Orientation, Heat ANK-191

Specimen No.	Test Temp., F	Asorbed Energy, ft-lb	Lateral Expagion, 10^{-3} in.	Shear Fracture, %
JJ-313	360	86	53	100
315	359	106	63	100
335	358	73	54	100
JJ-328	201	102	54	100
323	201	92	59	100
308	200	83	49	100
JJ-322	80	76	42	85
319	80	98	51	100
344	80	74	45	80
JJ-357	40	66	44	85
332	40	57	33	45
339	40	55	30	55
JJ-301	20	46	29	70
304	20	36	27	30
JJ-331	0	35	29	35
324	0	33	26	23
337	0	47	33	35
JJ-424	-59	27	20	2
420	-60	56	44	4
421	-61	67	35	6

Table C-4. Pre-Irradiation Charpy Impact Data for Shell Forging Material - HAZ, Transverse Orientation, Heat AWS-192

Specimen No.	Test Temp., F	Asorbed Energy, ft-lb	Lateral Expansion, 10 ⁻³ in.	Shear Fracture, %
KK-325	361	135	65	100
336	360	153	77	100
318	358	128	63	100
KK-343	278	118	76	100
339	278	125	76	100
344	277	132	76	100
KK-333	199	65	37	100
310	190	122	66	100
313	197	78	53	100
KK-346	139	131	77	100
337	139	132	67	100
348	139	121	71	100
KK-312	80	91	46	94
307	79	76	41	85
335	79	63	36	98
KK-308	40	141	67	100
316	40	72	42	35
327	40	66	40	45
KK-341	20	93	70	40
340	20	104	77	65
345	19	82	64	30
KK-317	0.5	106	64	45
324	0.1	43	31	18
326	0.1	43	32	40
KK-309	-40	30	22	20
330	-39	80	51	28
KK-342	-39	27	21	2
347	-40	52	35	5
338	-40	38	28	3

Table C-5. Pre-Irradiation Charpy Impact Data for Weld Metal WF-209-1

Specimen No.	Test Temp., F	Asorbed Energy, ft-lb	Lateral Expansion, 10^{-3} in.	Shear Fracture, %
JJ-063	359	57	49	100
083	357	58	48	100
089	357	65	53	100
JJ-091	201	57	46	100
053	201	63	50	100
084	199	78	57	100
JJ-093	140	60	46	100
060	140	69	52	100
065	140	61	49	100
JJ-092	110	64	46	100
038	110	58	46	100
077	109	47	37	96
JJ-064	80	61	40	98
095	80	38	32	95
081	79	48	35	85
JJ-090	40	28	28	10
069	40	33	29	15
075	40	21	20	12
JJ-061	-40	17	16	5
050	-40	16	14	2
057	-39	19	18	6

Figure C-1. Charpy Impact Data From Unirradiated Shell Forging Material (ANK-191), Transverse Orientation

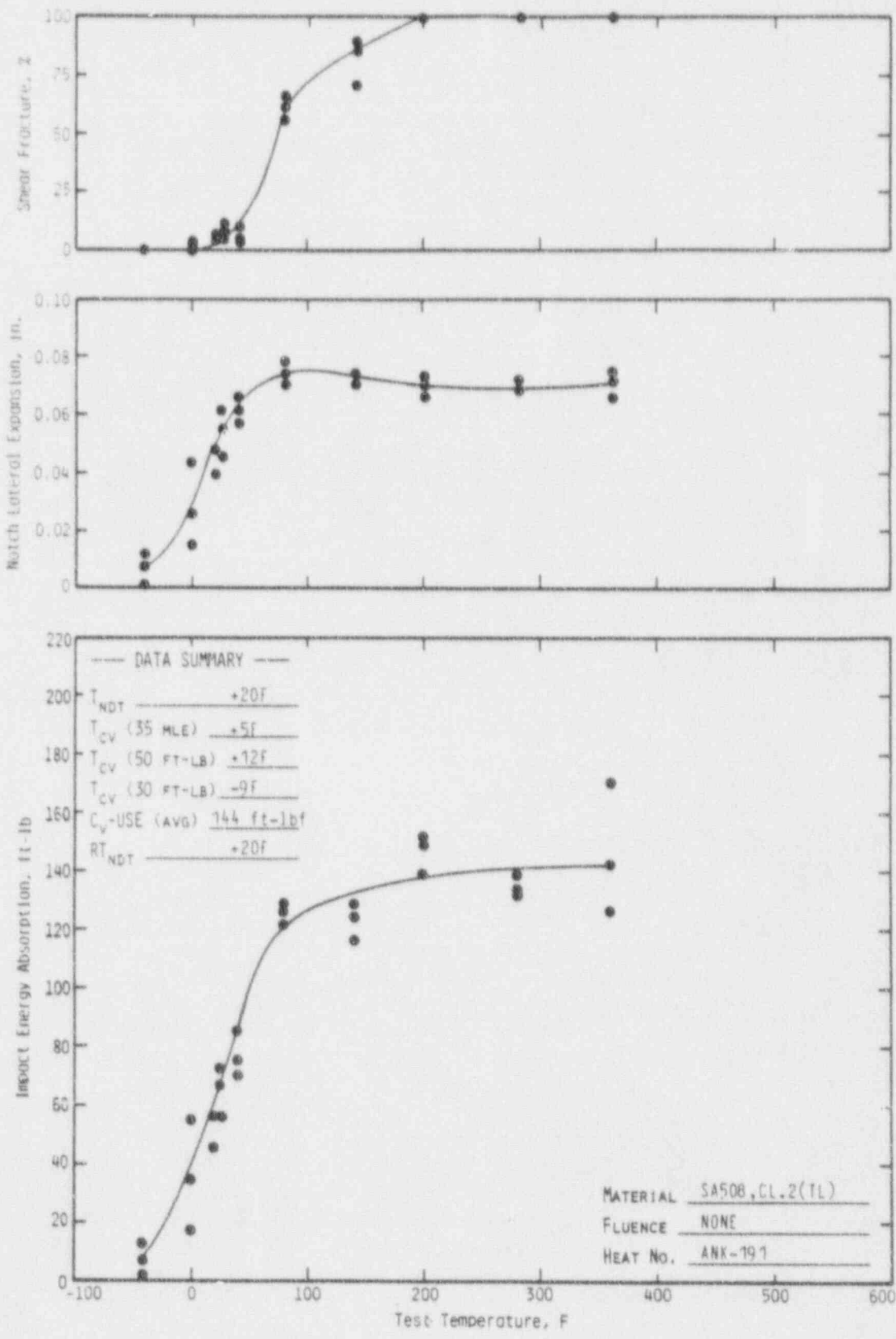


Figure C-2. Charpy Impact Data From Unirradiated Shell Forging Material (AWS-192), Transverse Orientation

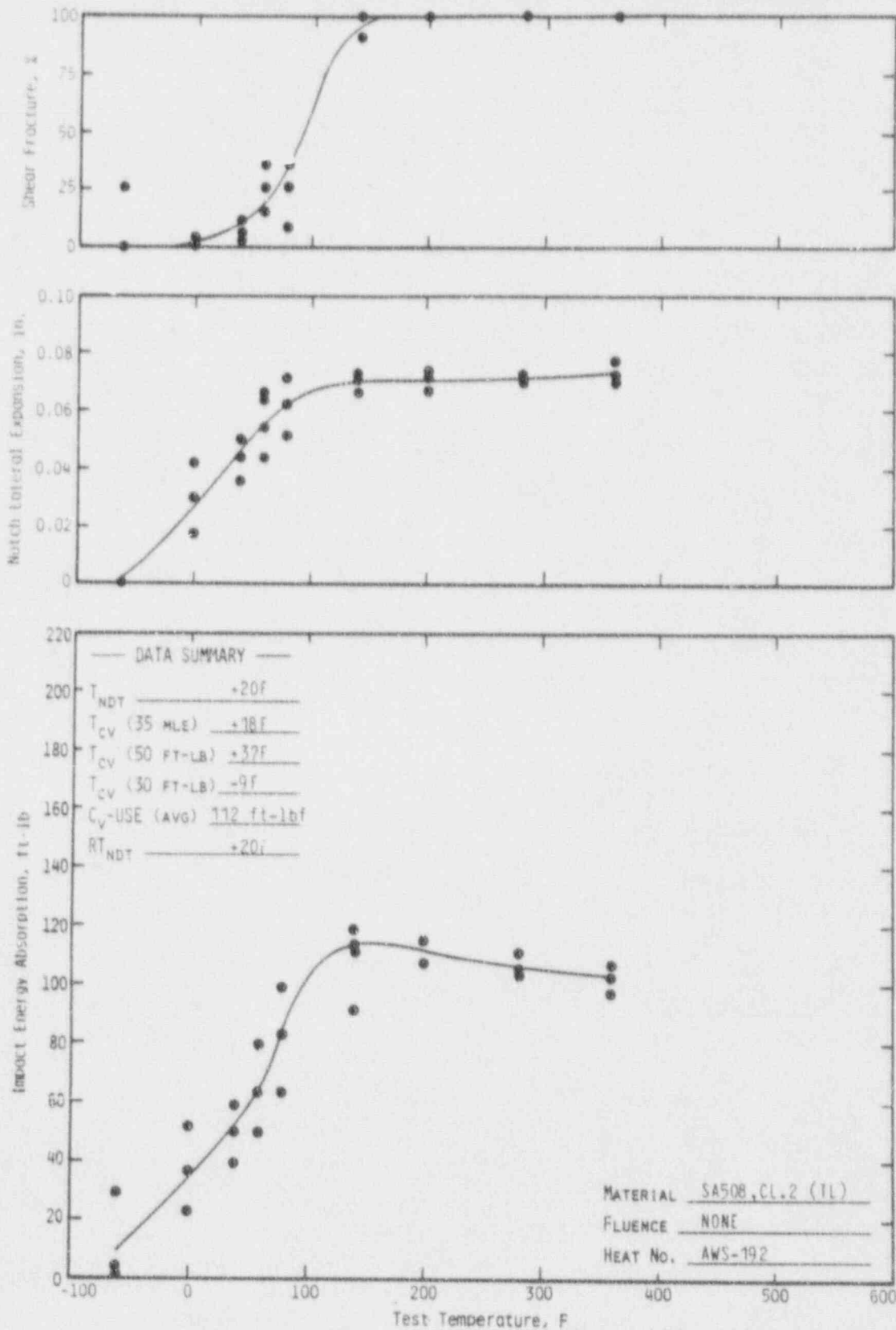


Figure C-3. Charpy Impact Data From Unirradiated Shell Forging Material (ANK-191) Heat-Affected Zone, Longitudinal Orientation

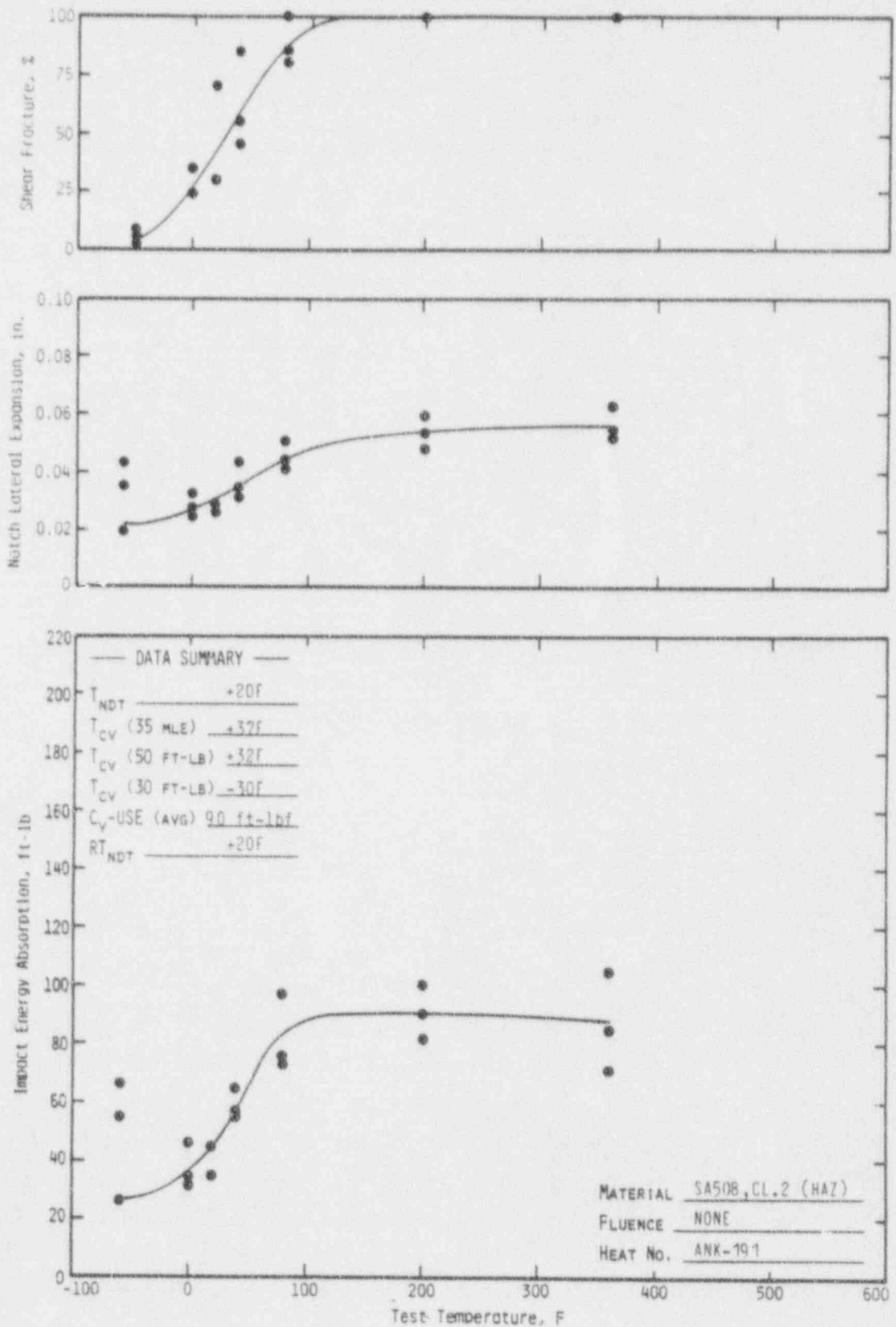


Figure C-4. Charpy Impact Data From Unirradiated Shell Forging Material (AWS-192) Heat-Affected Zone, Longitudinal Orientation

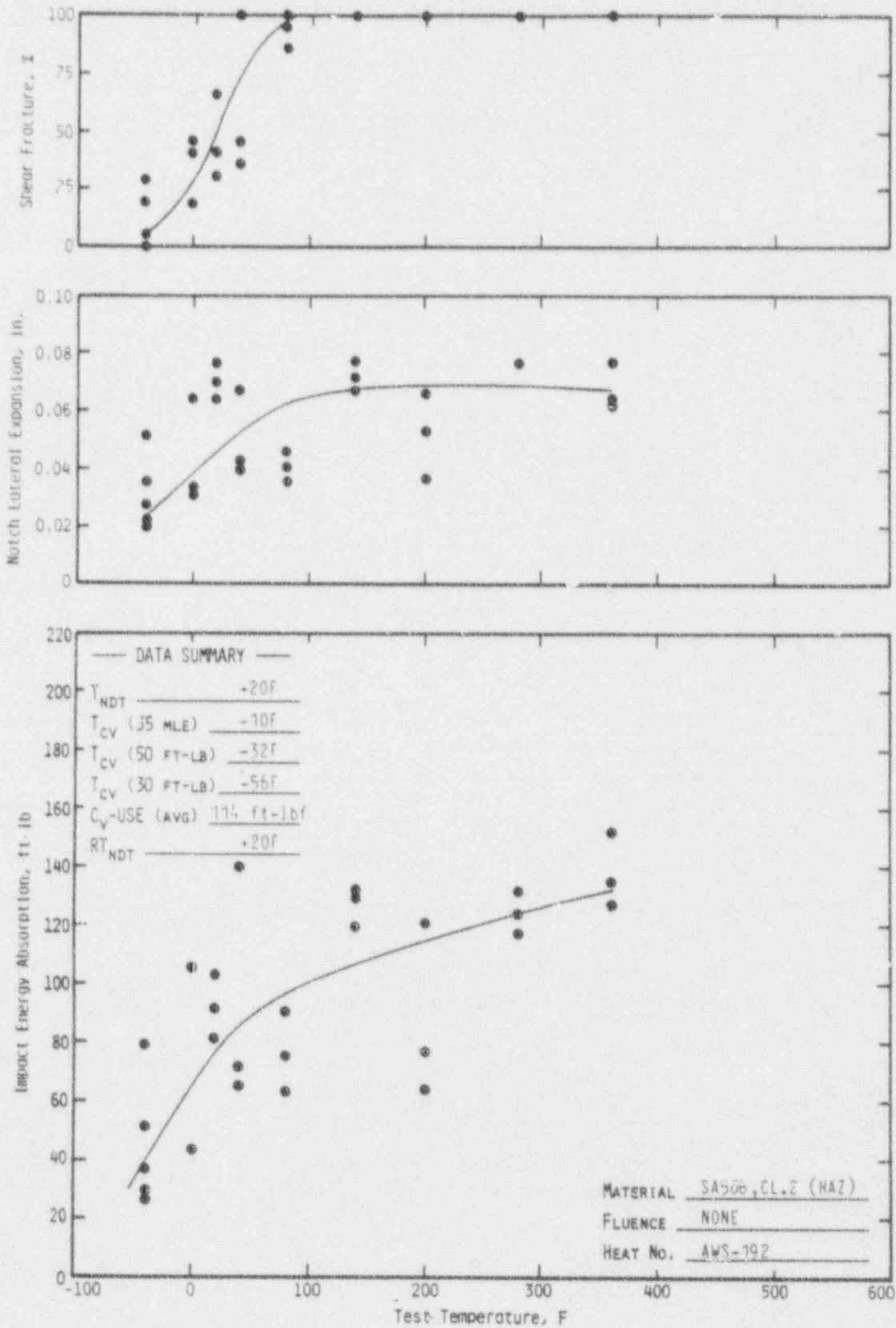
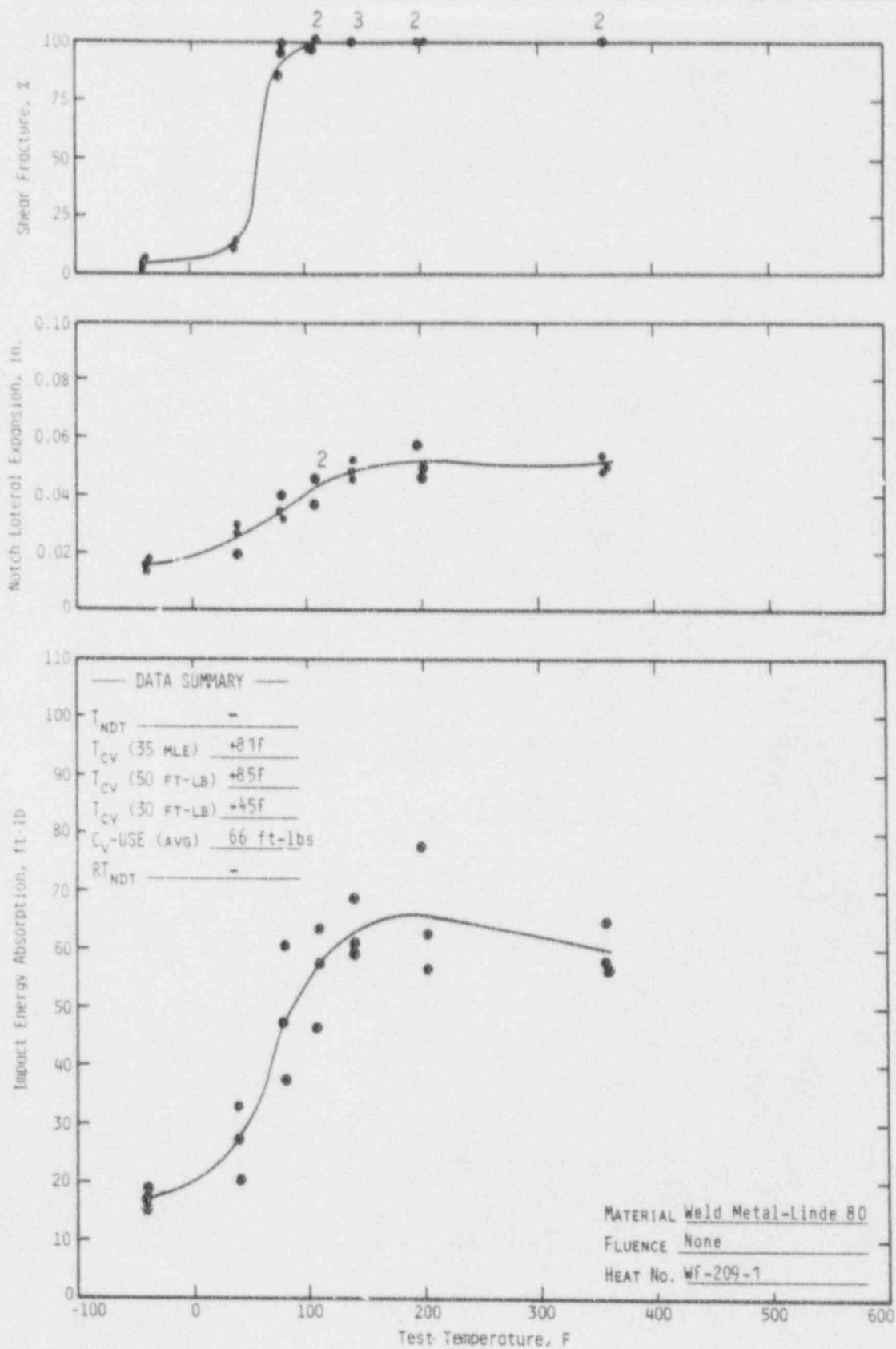


Figure C-5. Charpy Impact Data From Unirradiated Weld Metal, WF-209-1



APPENDIX D
Fluence Analysis Methodology

1. Analytical Method

A semiempirical method is used to calculate the capsule and vessel flux. The method employs explicit modeling of the reactor vessel and internals and uses an average core power distribution in the discrete ordinates transport code DOTIV, version 4.3. DOTIV calculates the energy and space dependent neutron flux for the specific reactor under consideration. This semiempirical method is conveniently outlined in Figures D-1 (capsule flux) and D-2 (vessel flux).

The two-dimensional transport code DOTIV was used to calculate the energy- and space-dependent neutron flux at all points of interest in the reactor system. DOTIV uses the discrete ordinates method of solution of the Boltzmann transport equation and has multi-group and asymmetric scattering capability. The reference calculational model is an R- θ geometric representation of a plan view through the reactor core midplane which includes the core, core liner, coolant, core barrel, thermal shield, pressure vessel, and concrete. The material and geometry model, represented in Figure D-3, uses one-eighth core symmetry. In order to include reasonable geometric detail within the computer memory limitations, the code parameters are specified as P₃ order of scattering, S₈ quadrature, and 22 energy groups. The P₃ order of scattering adequately describes the predominately forward scattering of neutrons observed in the deep penetration of steel and water media, as demonstrated by the close agreement between measured and calculated dosimeter activities. The S₈ symmetric quadrature has generally produced accurate results in discrete ordinates solutions for similar problems, and is used routinely in the B&W R- θ DOT analyses.

Flux generation in the core was represented by a fixed distributed source which the code derives based on a ²³⁵U fission spectrum, the input relative power distribution, and a normalization factor to adjust flux level to the desired power density.

Geometrical Configuration

For modeling purposes, the actual geometrical configuration is divided into three parts, as shown in Figure D-3. The first part, Model "A," is used to generate the energy-dependent angular flux at the inner boundary of Model "B," which begins at the outer surface of the core barrel. Model A includes a detailed

representation of the core baffle (or liner) in R- θ geometry that has been checked for both metal thickness and total metal volume to ensure that the DOT approximation to the actual geometry is as accurate as possible for these two very important parameters. The second, Model B, contains an explicit representation of the surveillance capsule and associated components. The B&W Owners Group's Flux Perturbation Experiment²² verified that the surveillance capsule must be explicitly included in the DOT models used for capsule and vessel flux calculations in order to obtain the desired accuracy. The magnitude of the perturbations in the fast flux due to the presence of the capsule was determined in the Perturbation Experiment to be as high as 47% at the capsule center and as high as 10% at the inner surface of the reactor vessel. Detailed explicit modeling of the capsule, capsule holder tube, and internal components is therefore incorporated into the DOT calculational models. The third, Model "C," is similar to Model B except that no capsule is included. Model C is used in determining the vessel flux in quadrants that do not contain a surveillance capsule; typically these quadrants contain the azimuthal flux peak on the inside surface of the reactor vessel.

An overlap region of approximately 32.5 cm or 17 radial intervals is specified between Model A and Models B or C. The width of this overlap region, which is fixed by the placement of the Model A vacuum boundary and the Model B boundary source, was determined by an iterative process that resulted in close agreement between the overlap region flux as predicted by Models A and B or C. The outer boundary was placed sufficiently far into the concrete shield (cavity wall) that the use of a "vacuum" boundary condition does not cause a perturbation in the flux at the points of interest.

Macroscopic Cross Sections

Macroscopic cross sections, required for transport analyses, are obtained with the mixing code GIP. Nominal compositions are used for the structural metals. Coolant compositions were determined using the average boron concentration over a fuel cycle and the bulk temperature of the region. The core region is a homogeneous mixture of fuel, fuel cladding, structure, and coolant.

The cross-section library presently used is the (22-neutron group and 18-gamma group) CASK 23E coupled set. The dosimeter reaction cross sections are based on the ENDF/B5 library, and are listed in Table E-3. The measured and calculated dosimeters activities are compared in Table D-1.

Distributed Source

The neutron population in the core during full power operation is a function of neutron energy, space, and time. The time dependence is accounted for in the analysis by calculating the time-weighted average neutron source, i.e. the neutron source corresponding to the time-weighted average power distribution. The effects of the other two independent variables, energy and space, are accounted for by using a finite but appropriately large number of discrete intervals in energy and space. In each of these intervals the neutron source is assumed to be invariant and independent of all other variables. The space and energy dependent source function can be considered as the product of a discretely expressed "spatial function" and a magnitude coefficient, i.e.

$$Sv_{ijg} = \underbrace{[\nu/K P_D]}_{\text{magnitude}} \times \underbrace{[RPD_{ij} X_g]}_{\text{spatial}} \quad (D-1)$$

where:

- Sv_{ijg} = Energy-and space-dependent neutron source, n/cc-sec,
- ν/K = Fission neutron production rate, n/w-sec,
- P_D = Average power density in core, w/cc,
- RPD_{ij} = Relative power density at interval (i,j), unitless,
- X_g = Fission spectrum, fraction of fission neutrons having energy in group "g,"
- i = Radial coordinate index,
- j = Azimuthal coordinate index,
- g = Energy group index.

The spatial dependence of the flux is directly related to the RPD distribution. Even though the entire (eighth-core symmetric) RPD distribution is modeled in the

analysis, only the peripheral fuel assemblies contribute significantly to the ex-core flux. The axial average pin-by-pin RPD distribution is calculated on a quarter-core symmetric basis for 8 to 12 times during each core cycle for the entire capsule irradiation period. The time-weighted average RPD distribution is used to generate the normalized space and energy dependency of the neutron source. Calculations for the energy and space dependent, time-averaged flux were performed for the midpoint of each DOT interval throughout the model. Since the reference model calculation produced fluxes in the R- θ plane that are averaged over the core height, an axial correction factor of 1.17 was required to adjust these fluxes to the capsule elevation.

1.1. Capsule Flux and Fluence Calculation

As discussed above, the DOTIV code was used to explicitly model the capsule assembly and to calculate the neutron flux as a function of energy within the capsule. The calculated fluxes were used in the following equation to obtain calculated activities for comparison with the measured data. The calculated activity for reaction product D_i , in ($\mu\text{Ci/gm}$) is:

$$D_i = \frac{N f_i}{(3.7 \times 10^4) A_n E} \sum \sigma_n (E) \phi(E) \sum_j F_j (1 - e^{-\lambda_i t_j}) e^{-\lambda_i (T - t_j)} \quad (D-2)$$

where:

N = Avogadro's number,

A_n = Atomic weight of target material n ,

f_i = Either weight fraction of target isotope in n -th material or the fission yield of the desired isotope,

$\sigma_n(E)$ = Group-averaged cross sections for material n (listed in Table E-3)

$\phi(E)$ = Group averaged fluxes calculated by DOTIV analysis,

F_j = Fraction of full power during j -th time interval, t_j

λ_i = Decay constant of the i th isotope,

T = Sum of total irradiation time, i.e., residual time in reactor,

and the wait time between reactor shutdown and counting times,

r_j = Cumulative time from reactor startup to end of j-th time period.

t_j = Length of the j-th time period

Adjustments were made to the calculated dosimeter activities to correct for the effects listed below:

Short half-life adjustments to Ni and Fe dosimeter activities

Photofission adjustments to ^{238}U and ^{237}Np dosimeter activities

Fissile impurity adjustments to ^{238}U dosimeter activities

After making these adjustments the calculated dosimeter activities were used with the corresponding measured activities to obtain the flux normalization factors:

$$C_i = \frac{D_i \text{ (measured)}}{D_i \text{ (calculated)}}$$

These normalization factors were evaluated, averaged, and then used to adjust the calculated test specimen flux and fluence to be consistent with the dosimeter measurements. Additionally, the normalization factor was used to update the average normalization factor which had been derived from previous analyses. The updated normalization factor was then used to adjust the calculated vessel flux and fluence. The flux normalization factors are given in Table D-1.

2. Vessel Fluence Extrapolation

For past core cycles, fluence values in the pressure vessel are calculated as described above. Extrapolation to future cycles is required to predict the useful vessel life. Three time periods are considered in the extrapolation: 1) operation to date for which vessel fluence has been calculated, 2) future fuel cycles for which PDQ calculations have been performed, and 3) future cycles for which no analyses exist.

For the Oconee Unit 3 analysis, time period 1 is through cycle 11, time period 2 covers cycles 12 and 13, and time period 3 covers from the end of cycle 13 through 32 EFPY. The flux and fluence for time period 2 was estimated by calculating the vessel flux using an adjoint-DOT calculational procedure with the appropriate assembly-average power distributions and integrating these values

over time period 2. The extrapolation of the fluence through time period 3 was accomplished by assuming that the average flux during period 3 was equal to the average flux for period 2 (cycles 12 and 13).

Table D-1. Flux Normalization Factor

	Measured Activity, (a) <u>μCi/g</u>	Calculated, Activity, (b) <u>μCi/g</u>	Flux Normalization Factor
$^{54}\text{Fe}(n,p)^{54}\text{Mn}$	935.27	1016.73	0.92 ^(c)
$^{58}\text{Ni}(n,p)^{58}\text{Co}$	1363.12	1397.86	0.98 ^(d)
$^{238}\text{U}(n,f)^{137}\text{Cs}$	18.35	17.29	1.06
$^{237}\text{Np}(n,f)^{137}\text{Cs}$	101.50	97.94	<u>1.04</u>
			Averaged: 1.00 ^(e)

(a) Average of four dosimeter wires.

(b) Average at four calculated activities.

(c) Average at four ratios (one for each dosimeter wire) corrected by short half-life factor of 0.83.

(d) Average of four ratios (one for each dosimeter wire) corrected by short half-life factor of 0.77.

(e) Average of all four dosimeters was selected as the normalization constant.

Table D-2. Oconee Unit 3 Reactor Vessel Fluence by Cycle

Cycles	Incremental Time, EFPY	Cumulative Time, EFPY	Vessel Flux, n/cm^2s	Vessel Fluence, n/cm^2 ^(c)	
				Incremental	Cumulative
1	1.31	1.31	1.39E+10	0.58E+18	0.58E+18
2-5	2.79	4.10	1.55E+10	1.37E+18	1.94E+18
6-11	6.56	10.66	9.49E+9	1.96E+18	3.91E+18
12	1.12	11.78	8.92E+9	3.16E+17	4.23E+18
13	1	12.91	7.62E+9 ^(a)	2.70E+17 ^(b)	4.50E+18 ^(b)
	2.09	15.00	8.27E+9 ^(a)	5.47E+17 ^(b)	5.05E+18 ^(b)
	6.00	21.00	8.27E+9 ^(a)	1.57E+18 ^(b)	6.62E+18 ^(b)
	3.00	24.00	8.27E+9 ^(a)	7.83E+17 ^(b)	7.40E+18 ^(b)
	8.00	32.00	8.27E+9 ^(a)	2.09E+18 ^(b)	9.49E+18 ^(b)

(a) The fuel cycle designs for future cycles 12 and 13 were used to estimate the maximum neutron flux at the inside surface of reactor vessel.

(b) Extrapolated values.

(c) Peak fluence at inside surface of reactor vessel.

Figure D-1. Rationale for the Calculation of Dosimeter Activities and Neutron Flux in the Capsule

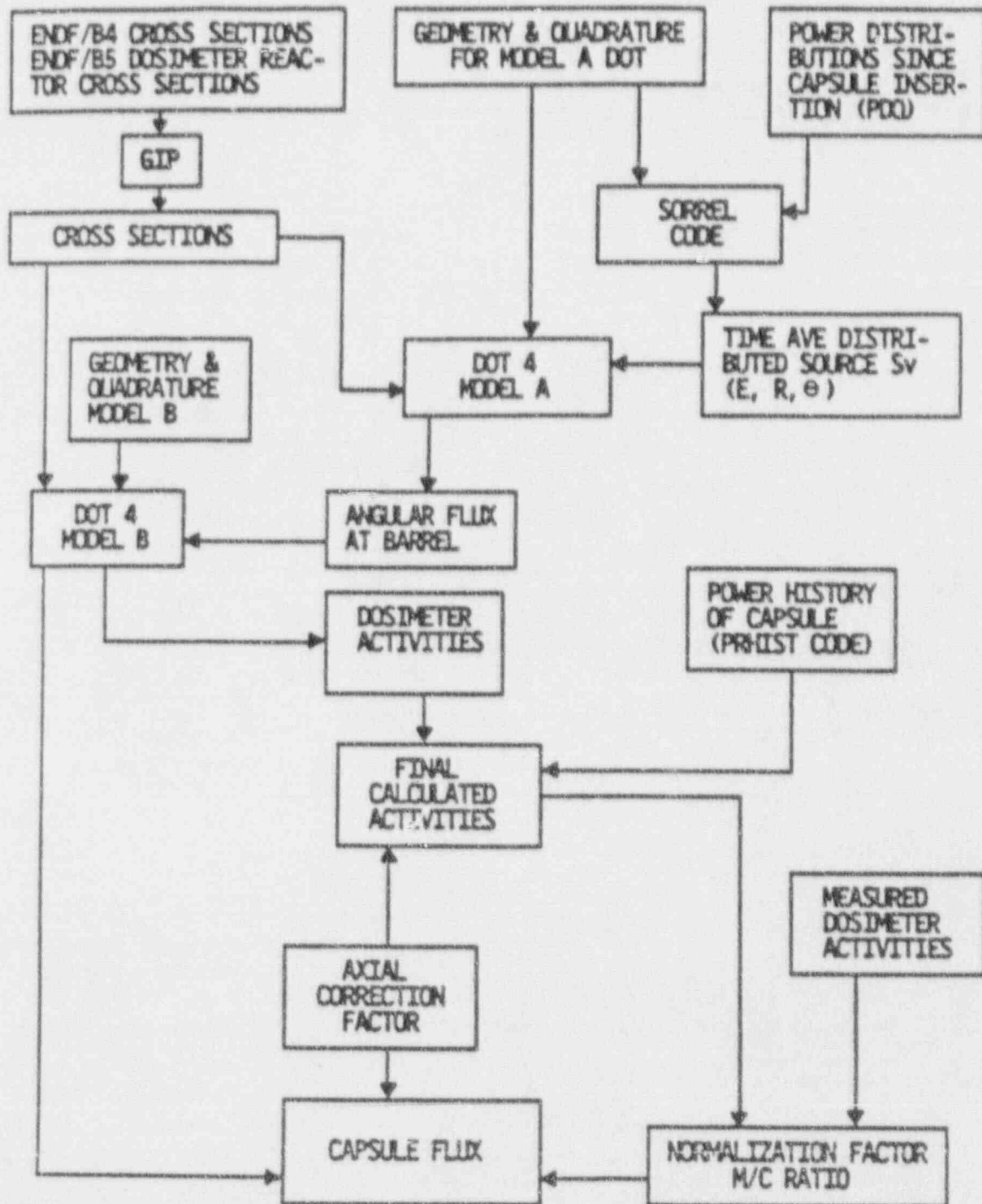


Figure D-2. Rationale for the Calculation of Neutron Flux in the Reactor Vessel

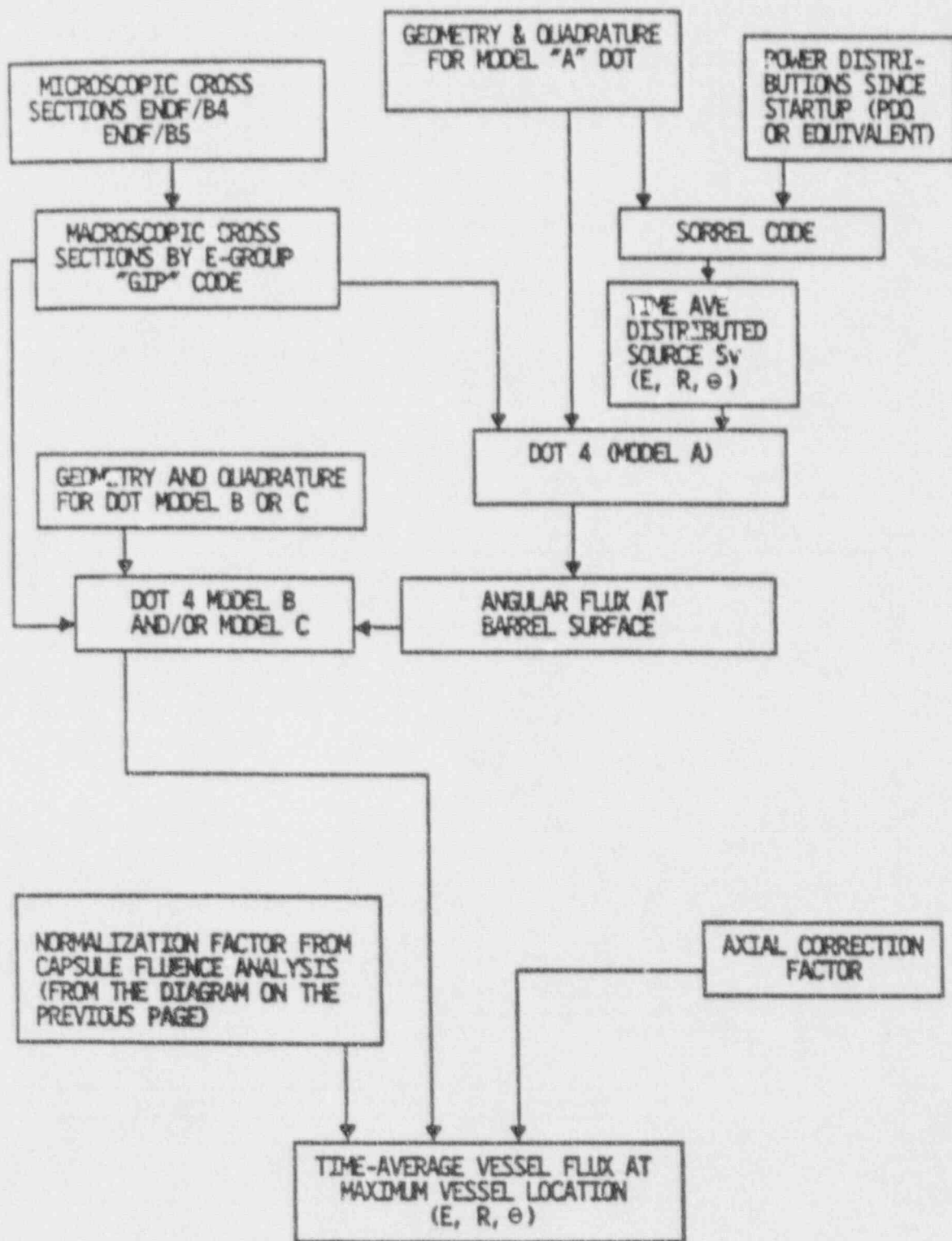
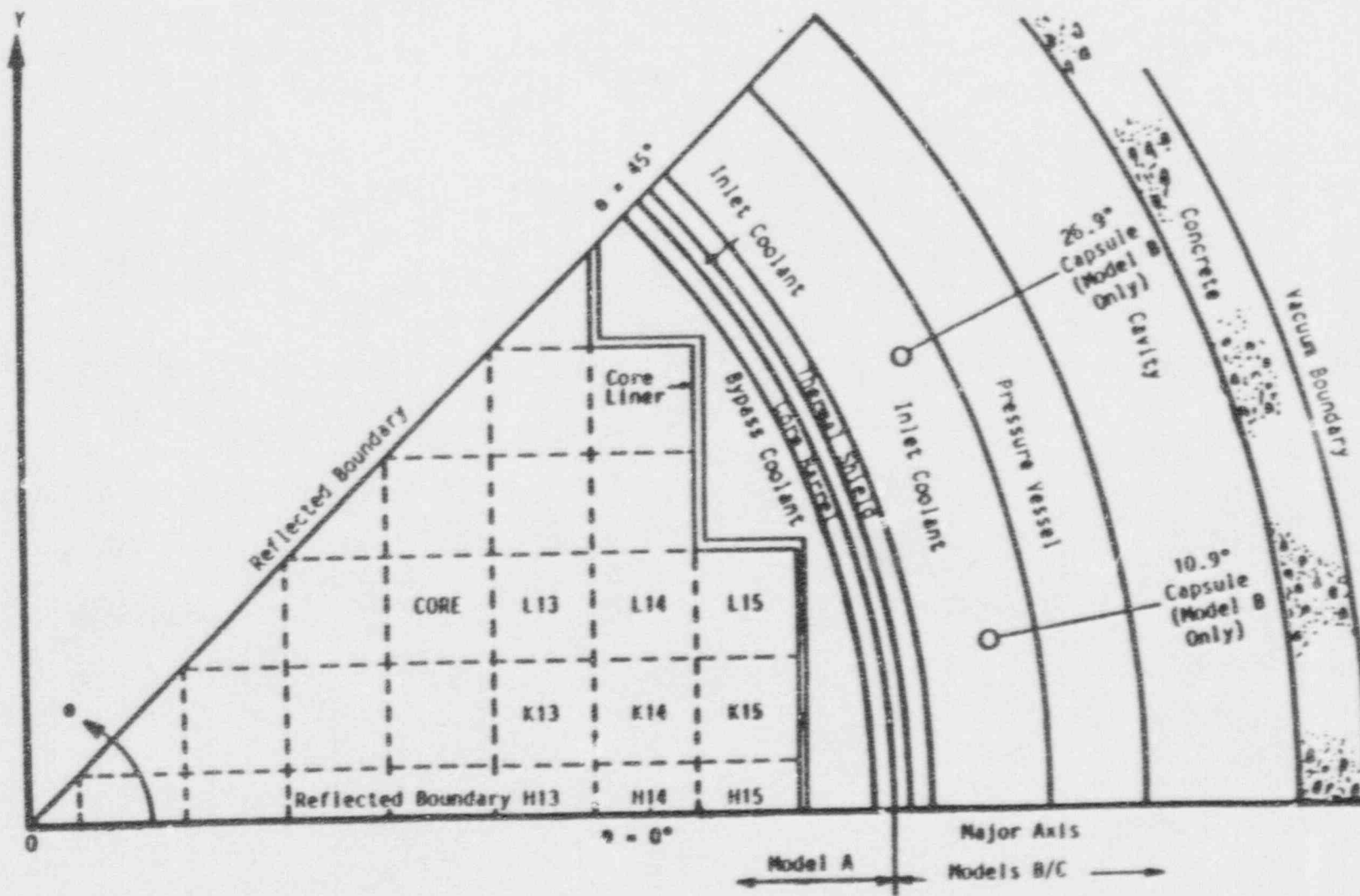


Figure D-3. Plan View Through Reactor Core Midplane
(Reference R-0 Calculation Model)



D-11

APPENDIX E
Capsule Dosimetry Data

Table E-1 lists the characteristics of the neutron dosimeters. Table E-2 shows the measured activity per gram of target material (i.e., per gram of uranium, nickel, etc.) for the capsule dosimeters. Activation cross sections for the various materials were flux-weighted with the ^{235}U fission spectrum shown in Table E-3.

Table E-1. Detector Composition and Shielding

<u>Detector Material</u>	<u>% Target</u>	<u>Shielding</u>	<u>Reaction</u>
U-Al	10.38% ^{238}U	Cd-Ag	$^{238}\text{U}(n, f)^{137}\text{Cs}$
Np-Al	1.44% ^{237}Np	Cd-Ag	$^{237}\text{Np}(n, f)^{137}\text{Cs}$
Ni	67.77% ^{58}Ni	Cd-Ag	$^{58}\text{Ni}(n, p)^{58}\text{Co}$
Co-Al	0.66% ^{59}Co	Cd	$^{59}\text{Co}(n, \gamma)^{60}\text{Co}$
Co-Al	0.66% ^{59}Co	None	$^{59}\text{Co}(n, \gamma)^{60}\text{Co}$
Fe	5.82% ^{54}Fe	None	$^{54}\text{Fe}(n, p)^{54}\text{Mn}$

Table E-2. Measured Specific Activities (Unadjusted)
for Dosimeters in Capsule OC3-D

<u>Detector Material</u>	<u>Dosimeter Reaction</u>	<u>Dosimeter Activity, ($\mu\text{Ci/gm of Target}$)</u>			
		<u>DD5</u>	<u>DD6</u>	<u>DD7</u>	<u>DD8</u>
Ni	$^{58}\text{Ni}(n, p)^{58}\text{Co}$	1252.84	1725.77	1196.49	1640.06
Fe	$^{54}\text{Fe}(n, p)^{54}\text{Mn}$	802.15	1091.91	812.36	1034.64
U-Al	$^{238}\text{U}(n, f)^{137}\text{Cs}$	15.44	22.20	14.81	20.94
Np-Al	$^{237}\text{Np}(n, f)^{137}\text{Cs}$	89.98	120.64	85.60	109.74

Table E-3. Dosimeter Activation Cross Sections, b/atom(a)

G	Energy Range, MeV	$^{237}\text{Np}(n,f)$	$^{238}\text{U}(n,f)$	$^{58}\text{Ni}(n,p)$	$^{54}\text{Fe}(n,p)$
1	12.2 - 15	2.323	1.051E+0	4.830E-1	4.133E-1
2	10.0 - 12.2	2.341	9.851E-1	5.735E-1	4.728E-1
3	8.18 - 10.0	2.309	9.935E-1	5.981E-1	4.772E-1
4	6.36 - 8.18	2.093	9.110E-1	5.921E-1	4.714E-1
5	4.96 - 6.36	1.542	5.777E-1	5.223E-1	4.321E-1
6	4.06 - 4.96	1.532	5.454E-1	4.146E-1	3.275E-1
7	3.01 - 4.06	1.614	5.340E-1	2.701E-1	2.193E-1
8	2.46 - 3.01	1.689	5.325E-1	1.445E-1	1.080E-1
9	2.35 - 2.46	1.695	5.399E-1	9.154E-2	5.613E-2
10	1.83 - 2.35	1.676	5.323E-1	4.856E-2	2.940E-2
11	1.11 - 1.83	1.59 ^c	2.608E-1	1.180E-2	2.948E-3
12	0.55 - 1.11	1.241	9.845E-3	1.336E-3	6.999E-5
13	0.111 - 0.55	2.352E-1	2.436E-4	5.013E-4	6.419E-8
14	0.0033 - 0.111	1.200E-2	6.818E-5	1.512E-5	0

(a) ENDF/B5 values that have been flux weighted (over CASK energy groups) based on a ^{235}U fission spectrum in the fast energy range plus a 1/E shape in the intermediate energy range.

APPENDIX F
References

1. A. L. Lowe, Jr., et al., Integrated Reactor Vessel Material Surveillance Program, BAW-1543A, Rev. 2, Babcock & Wilcox, Lynchburg, Virginia, May 1985, and Addendum 1, July 1987.
2. A. L. Lowe, Jr., et al., Analyses of Capsule OCIII-A from Duke Power Company Oconee Unit-3, Reactor Vessel Materials Surveillance Program, BAW-1438, Babcock & Wilcox, Lynchburg, Virginia, July 1977.
3. A. L. Lowe, Jr., et al., Analyses of Capsule OCIII-B from Duke Power Company Oconee Nuclear Station Unit-2, Reactor Vessel Materials Surveillance Program, BAW-1697, Babcock & Wilcox, Lynchburg, Virginia, October 1981.
4. G. J. Snyder and G. S. Carter, Reactor Vessel Material Surveillance Program, Revision 3, BAW-10006A, Revision 3, Babcock & Wilcox, Lynchburg, Virginia, January 1975.
5. American Society for Testing and Materials, Recommended Practice for Surveillance Tests on Structural Materials in Nuclear Reactors, E185-66, November 1966.
6. Code of Federal Regulation, Title 10, Part 50, Fracture Toughness Requirements for Light-Water Nuclear Power Reactors, Appendix G, Fracture Toughness Requirements.
7. Code of Federal Regulation, Title 10, Part 50, Fracture Toughness Requirements for Light-Water Nuclear Power Reactors, Appendix H, Reactor Vessel Material Surveillance Program Requirements.
8. American Society of Mechanical Engineers (ASME) Boiler and Pressure Vessel Code, Section III, Nuclear Power Plant Components, Appendix G, Protection Against Nonductile Failure (G-2000).
9. Heavy Section Steel Technology Program, Semiannual Progress Report for Period Ending February 28, 1969, ORNL-4463, Oak Ridge National Laboratory, Oak Ridge, Tennessee, January 1970.
10. American Society for Testing and Materials, Methods and Definitions for Mechanical Testing of Steel Products, A370-77, June 24, 1977.

11. American Society for Testing and Materials, Methods for Notched Bar Impact Testing of Metallic Materials, E23-82, March 5, 1982.
12. S. Q. King, Pressure Vessel Fluence Analysis for 177-FA Reactors, BAW-1485P, Revision 1, Babcock & Wilcox, Lynchburg, Va., April 1988.
13. B&W's Version of DOTIV Version 4.3, One- and Two-Dimensional Transport Code System," Oak Ridge National Laboratory, Distributed by the Radiation Shielding Information Center as CC-429, November 1, 1983.
14. "CASK-40-Group Coupled Neutron and Gamma-Ray Cross Section Data," Radiation Shielding Information Center, DLC-23E.
15. Dosimeter File ENDF/B5 Tape 531, distributed March 1984, National Neutron Data Center, Brookhaven National Laboratory, Upton, Long Island, NY.
16. American Society of Testing Materials, Characterizing Neutron Exposures in Ferritic Steels in Terms of Displacements Per Atom (DPA), E693-79 (Reapproved 1985).
17. U.S. Nuclear Regulatory Commission, Radiation Damage to Reactor Vessel Material, Regulatory Guide 1.99, Revision 2, May 1988.
18. A. L. Lowe, Jr. and J. W. Pegram, Correlations for Predicting the Effects of Neutron Radiation on Linde 80 Submerged-Arc Welds, BAW-1803, Revision 1, B&W Nuclear Service Company, Lynchburg, Virginia, March 1991.
19. H. W. Behnke, et al., Methods of Compliance With Fracture Toughness and Operational Requirements of Appendix G to 10CFR50, BAW-10046A, Rev. 2, Babcock & Wilcox, Lynchburg, Virginia, June 1986.
20. J. D. Aadland, Babcock & Wilcox Owner's Group 177-Fuel Assembly Reactor Vessel and Surveillance Program Materials Information, BAW-1820, Babcock & Wilcox, Lynchburg, Virginia, December 1984.
21. K. E. Moore and A. S. Heller, B&W 177-FA Reactor Vessel Beltline Weld Chemistry Study, BAW-1799, Babcock & Wilcox, Lynchburg, Virginia, July 1983.

22. N. L. Snider and L. A. Hassler, B&WOG Flux Perturbation Experiment at ORNL, Measured and Calculated Dosimeter Results, BAW-1886, Babcock & Wilcox, Lynchburg, Virginia, September 1985.